Journal of Environmental Management 344 (2023) 118493

Contents lists available at ScienceDirect

Journal of Environmental Management

journal homepage: www.elsevier.com/locate/jenvman

Research article

Seasonal differences in trace metal concentrations in the major rivers of the hyper-arid southwestern Andes basins of Peru

Alexander Ccanccapa-Cartagena [a,c,*], Francisco D. Chavez-Gonzales [b,e], Betty Paredes [b], Corina Vera [b], Guillermo Gutierrez [d], Roland Valencia [e], Ana Lucia Paz Alcázar [f], Nadezhda N. Zyaykina [a,h], Timothy R. Filley [g], Chad T. Jafvert [a,h]

[a] Lyles School of Civil Engineering, Purdue University, West Lafayette, 47907 IN, USA
[b] Departamento de Química, Independencia Av. S/N, Universidad Nacional de San Agustín, Arequipa, 04000, Peru
[c] Escuela Profesional de Antropología, Universidad Nacional de San Agustín de Arequipa, Av. Venezuela S/N, 04000, Arequipa, Peru
[d] Servicio Nacional de Meteorología e Hidrología del Perú, Dirección Zonal 6, Arequipa, 04000, Peru
[e] Autoridad Nacional del Agua del Peru, AAA Caplina-Ocoña, Arequipa, 04000, Peru
[f] Autoridad Autónoma de Majes, Arequipa, 04000, Peru
[g] Department of Earth & Atmospheric and Planetary Sciences, Purdue University, West Lafayette, 47907 IN, USA
[h] Environmental and Ecological Engineering, Purdue University, West Lafayette, 47907 IN, USA

ARTICLE INFO

Keywords:
Arequipa
Seasonality
Dissolved metals
Total metals
Geogenic
Anthropogenic
Monitoring

ABSTRACT

The southern rivers of Peru originate in the Andes Mountains and flow in a southwestern direction to the Pacific Ocean through one of the most hyper-arid regions of the world. During each sub-equatorial summer from December to February, rains and snow melt in the Andes increase the streamflow in these rivers, even as they pass through the 100 km arid zone to the ocean. This study quantified seasonal dynamics of 34 trace metal elements (TM) and other constituent concentrations in four southern river basins of Peru (Chili-Quilca, Tambo, Camana-Majes-Colca, and Ocoña) during 2019–2020. Consistent with previous studies, we observed that: (1) the river water in the southern basins had relatively high concentrations of B, As, Fe, Al, Mn, P, Pb and Ni, with As the most ubiquitous toxic TM in all the basins, often detected at concentrations surpassing Peruvian and USEPA regulated concentrations; and (2) basins with the most to least toxic TM contamination were the Tambo > Chili-Quilca > Camana-Majes-Colca > Ocoña. Seasonal streamflow strongly influenced the concentrations of twenty TM, with 15 TM (Al, Au, Ba, Cd, Co, Cu, Fe, Gd, Mn, Ni, P, Pb, Ti, Yb and Zr) consistently higher in the wet season, and with As, B, Ge, Li, and Pd higher in the dry season. Our results improve the understanding of seasonal variability and vulnerability in western Andes superficial water sources, which are highly influenced by both local geogenic and anthropogenic conditions. A Spanish translation of this paper is available in the online Supplementary Material.

1. Introduction

Pollution of freshwater rivers is a critical issue as the demand for access to clean water sources has increased because of increases in regional populations and economic activities (e.g., mining and other industrial activities, agriculture, hydropower, tourism, etc.) (Reza and Singh, 2010; Liu et al., 2019a). TM contamination has long been a concern since it is directly related to human and environmental health, and continued economic development (Li et al., 2008; Jiajun et al., 2014; Singh and Kumar, 2017). The contamination of rivers by TM can significantly affect the functioning of river systems, as well as sustainable development and hydraulic performance (Walaszek et al., 2018; Adams et al., 2020). The presence of TM can have a considerable impact on biota, drinking water supplies, soil and sediment quality. Furthermore, hydraulic systems are susceptible to the impacts of TM contamination through processes such as settling, filtering, and bioassimilation by microorganisms. The consequences of TM contamination can be far-reaching for both the natural environment and human health, especially in developing regions such as Asia, Africa, and South America (Chowdhury et al., 2016; Nthunya et al., 2017; Alves et al., 2019). Toxic

* Corresponding author. Lyles School of Civil Engineering, Purdue University, West Lafayette, 47907 IN, USA.
E-mail address: ccanccap@uv.es (A. Ccanccapa-Cartagena).

https://doi.org/10.1016/j.jenvman.2023.118493
Received 5 February 2023; Received in revised form 15 June 2023; Accepted 21 June 2023
Available online 24 July 2023

TM contamination results not only from natural processes, such as mineral weathering and erosion, but also from industrial activities, such as dumping of TM waste, mining activities, disposal of sewage sludges, and excessive use of chemical fertilizers and pesticides (Mansoor et al., 2018; Kumar et al., 2019; Liu et al., 2019b; Adams et al., 2020). The contributions of these sources are different in different regions and in different seasons. Combined with seasonal differences in rainfall and snowmelt, heavy TM concentrations in surface waters can vary both seasonally and spatially (Xiaolong et al., 2010; Saleem et al., 2019).

In aquatic ecosystems, sediments are often a sink for TM, however when physical disturbances (e.g. seasonal flow variations), or changes in pH or redox conditions occur, these sediments can become a source of TM, releasing them in the overlying water column and affecting the ecosystem (Nyantakyi et al., 2019). Indeed, changes in flow or other conditions affect overall sedimentation processes including the sequestration and release of TM species (Mohiuddin et al., 2012; Wang et al., 2018). Thus, understanding the seasonal variability in surface water quantity (i.e., flow) and quality is key to fully understanding risks associated with natural and anthropogenic sources of contamination.

The Andes Mountains dominate the central north to south corridor of Peru, and are a natural reserve of transition metals and metalloids, where intensive mining activities (legal and small scale informal) occur (Bebbington and Bury, 2009; Geological Survey, 2018). Additionally, in southern Peru, geothermal features, which include several active volcanos, are potential sources of TM, contributing to the contamination of the rivers located on the western slopes of the Andes. These rivers flow from the Andes through the hyper-arid region along the coast, that has a mean annual precipitation of 15 mm (Garreaud, 2009; Viale et al., 2019).

There are several studies in the literature that report seasonal trends of dissolved metal concentrations in various rivers around the world (Caccia and Millero, 2003; Li and Zhang, 2010; Mohiuddin et al., 2012; Kumar et al., 2013; Wang et al., 2018; Hossain et al., 2020). However, there are few studies that have monitored both dissolved and total recoverable metal concentrations (Gozzard et al., 2011). Because increased suspended solid concentrations often occur during high flows, the concentration of dissolved metals may under-estimate the total metal concentration, and hence under-estimate the mass flux of TM in the water body. Indeed, dissolved and total metal concentrations and flow data are required to determine the real impact of TM pollution to downstream ecosystems.

Several studies report on TM concentrations in river basins in Peru, mainly in the north and central regions, concentrating on toxicity assessment and spatial distribution within the basins, with no study reporting on seasonal (temporal) trends, especially as a function of stream flow (Yacoub et al., 2013; Barenys et al., 2014; Cabrera et al., 2017; de Meyer et al., 2017; Terrazas et al., 2017; Grande et al., 2019). Indeed, to our knowledge, there are limited studies on seasonal TM concentrations in rivers in Perú (Guittard et al., 2020; Pari-Huaquisto et al., 2020). Yet, Peru's hydro-climate is one of the most extreme and vulnerable (to climate change) in the world, with the presence of two marked seasons within the western Andes and hyper-arid coastal region (Garreaud, 2009). Hence, the primary objective of this study was to investigate the seasonal variations in dissolved and total metal concentrations in four river basins located on the southeastern slope of the Andes mountains in the Arequipa region of Peru. Possible sources of these TM in the wet and dry seasons also are discussed. For this purpose, 18 sites across the four river basins were sampled 4 times over 12 months, resulting in 72 surface water samples collected in three dry months (March, July and October of 2019) and in the wet mouth of February (in 2020). Both dissolved and total metal concentrations were measured in all samples, measuring 38 TM in each sample, resulting in over 5000 discrete data points.

2. Materials and methods

2.1. Study area and hydro-climate

The study area is located in the Arequipa region of Peru, approximately 600–800 km southeast of Lima, stretching from the Ocoña River in the Northwest, to the Tambo River in the Southeast. The climate is influenced by the presence of the Andes, by the Humboldt Current System (HCS), by trade winds and El Niño-Southern Oscillation (ENSO) cycle. Annually, the HCS has an impacting cooling influence on Pacific Ocean of Peru. It is also responsible for the dryness of the coastal area since the current cools the marine air which, in turn, causes little or no precipitation during summer, otherwise higher precipitation occurs in the mountains Andes and Amazon Forest areas (Garreaud, 2009; Sepulchre et al., 2009; Perry et al., 2014). This region is the largest minerals production area in Peru (Ministerio de Enegia y Minas, 2019) and its geography is dominated by the Western Andes Mountains in the Northeast, to the Atacama desert in the Southwest, which is one of the driest deserts of the world. This region contains several active volcanos (Fabre et al., 2006; Gałaś, 2014). Anthropogenic activities, volcanic and other natural activities, and the regional hydroclimate all influence the concentrations of metal cations and metalloid oxyanions found within the rivers of these basins.

Note that historically, the names of rivers in Peru often change when the river enters a new urban area, without convergence of a tributary occurring. For example, the Chili river becomes the Vítor River near the town of Vítor, and later becomes the Quilca as it approaches the town of Quilca, near its confluence at the Pacific Ocean. Hence, for clarity the river basins are named after the major reaches of the watershed. The Chili-Quilca, Camana-Majes-Colca, Tambo, and Ocoña River basins (Fig. 1 and Figure S-1) flow through the hyper-arid west coast of Peru, and have cut deep but narrow fertile valleys from the Andes to the Pacific Ocean. In the Chili-Quilca watershed lies the second largest city of Peru, Arequipa. In the Colca basin, the altitude drops from 4886 m at the head of the watershed to sea level at the Pacific Ocean. In the desert region, several extensive gravity-fed irrigation districts exist, including the Majes (23,000 ha) and La Joya (8000 ha) districts. In addition to irrigating the fields, the water is used by the farmers and others who work and live in these irrigation districts for household needs, including as their potable water source.

The hydro-climate of southwestern Peru is characterized by two annual seasons: a dry season (late March to November) and a wet season (December to February) (Garreaud, 2009). Additionally, the annual mean precipitation varies depending on the altitude within each basin. For instance, the Chili-Quilca basin has landscapes at 4000 m (Imata) with an annual mean precipitation of 5.19 m, whereas at 1255 m (La Joya) the annual precipitation is only 0.0018 m, similar to that at sea level at the mouth of the Quilca River. Within the Camana-Majes-Colca basin, at an elevation of 4410 m (Dique de los españoles, Caylloma) the annual precipitation is 5.65 m, whereas at an elevation of 645 m (Majes) in the same basin, the annual precipitation is only 0.0048 m. Meanwhile, the Tambo and Ocoña basins, the annual mean precipitation is 1.5 and 3.9 m, respectively. Due to the climate cycle, in which both high precipitation and glacial snowmelt occur during the same season, the average flow in the Chili-Quilca basin fluctuates from approximately 4 to 8 m^3/s during the dry season to more than 80 m^3/s during the wet season (Montesinos-Tubée et al., 2019); in the Camana-Majes-Colca basin, the variation is less severe from 83 to 241 m^3/s; in the Tambo basin, flows vary from 31 to 399 m^3/s; and in the Ocoña basin, the flows vary from 51 to 302 m^3/s (UNESCO, 2006) from dry to wet seasons, respectively.

2.2. Sampling sites and sample analysis

Eighteen sampling sites were selected based on previous water quality sampling by the National Authority of Water of Peru (ANA). Sites

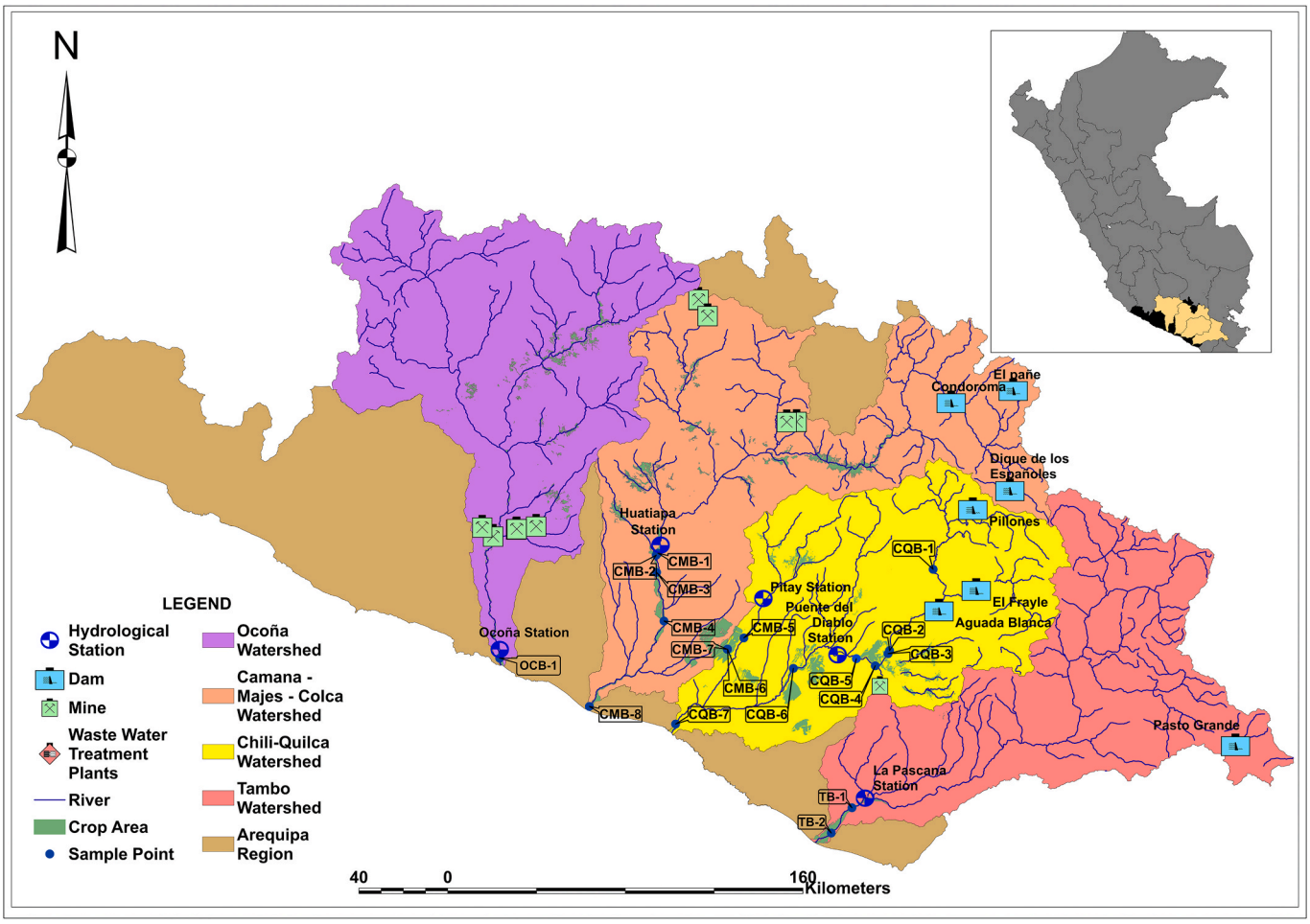

Fig. 1. Map of sampling site monitoring at Arequipa Region basin.

were on the Chili-Quilca (7 sites), Camana-Majes-Colca (8, 6 river samples and 2 retention ponds samples), Tambo (2) and Ocoña (1) rivers. Water samples were collected during the dry and wet periods. Dry period samples were collected in March, July, and October of 2019 and wet period samples were collected in February of 2020. During each of the four sampling events, 18 discrete samples (in triplicate) were collected, for a total of 72 samples.

All water samples were collected following the method described by Chapman et al. (1996). In summary, a plastic sampling container was rinsed three times with stream water at the sampling location prior to sample collection. The samples were taken at a depth of 0–20 cm from the water surface with the mouth of the 1 L container pointing against the direction of flow. After transferring triplicate samples to 50 mL metal-free polypropylene centrifuge tubes (VWR), the remaining water in the container was analyzed in the field for temperature, pH, electrical conductivity (EC), and total dissolved solids (TDS) using a portable Hanna H198129 tester with pre-calibrated probes. All sample tubes were shipped or transported to Purdue University (USA) for TM analysis. Because of international shipping regulations, the regular sampling protocol varied slightly in this study, causing a delay between sample collection and sample acidification. To overcome this modification, additional steps were followed, including sample shaking and sonication to solubilize metals before filtering an aliquot through a syringe disk filter (SFCA, 0.45 μm) for dissolved metal analysis. The filtrate was acidified with concentrated nitric acid (trace metal grade, Fisher Scientific) to 2%. For total recoverable metal analysis, another of the 50 mL triplicate samples from each sampling site (unfiltered) was acidified to 2% HNO3, and then centrifugated at 10,000 rpm for 20 min. Finally, 15 mL of the resulting supernatant was collected for TM analysis. To support the results consistency (because of the preservation step limitation), metal concentration results in this study were compared to those available from water quality monitoring reports provided by the National Water Authority ((https://www.ana.gob.pe/). These reports include data on inorganic (eighteen metals) and organic contaminants, as well as several physico-chemical water parameters. Our results were consistent with historical values reported from 2011 to 2018 (Tables S–7) for the southern basins. Additional information in detail about sample treatment can be found in SI-1 and quality assurance and quality control and instrumentation in SI-2.

2.3. Statistical analysis

IBM SPSS version 22.0 (SPSS Inc., Chicago, IL, USA) was used for statistical analyses including multivariate analyses (hierarchical cluster analysis and principal component analysis/factor analysis) to determinate the source of TM in each season. Multivariate statistical methods, such as principal component analysis (PCA), are generally employed for pattern recognition, classification, and data dimensionality reduction. PCA has been applied successfully to environmental parameters from aquatic systems to identify potential sources of trace elements (natural versus anthropogenic) (DelValls et al., 1998; Ccanccapa-Cartagena et al., 2021). In the current study, PCA was conducted on the normalized data sets for each season, on 30 and 35 variables in the dry and wet seasons, respectively. Significant factors were selected based on the Kaiser principle of accepting factors with eigenvalues >1. Factor loadings were considered significant if they were >0.6 (DelValls et al.,

1998). Varimax rotation was used to maximize the sum of the variance of the factor coefficients. Hierarchical cluster analysis (CA) was performed on seasonal dataset (dry and wet) of TM to group the TM using Ward's method with Euclidean distances as measure of similarity (Nguyen et al., 2020).

The statistical analysis showed that the data were non-normally distributed, therefore subjected to nonparametric tests. Kendall rank correlation was performed to observe the association among the TM and the physical chemical parameters (R-Studio software) (Bashir et al., 2020).

Spearman non-parametric correlation coefficient, between TM concentrations and water flows, was performed to determine possible relationships among them. To perform the Spearman evaluation, each season was transformed to a numerical value in the data file (dry season = 1 and wet season = 2) (Allafta and Opp, 2020). This numerical variable was then correlated (pair by pair) with all the measured parameters. Furthermore, the mean for each of the parameters were calculated for each season and the result obtained were statistically analyzed using the paired sample student t-test.

3. Results and discussion

3.1. Physical characteristics of the southern basins

Table 1 shows the average values of temperature, conductivity, pH, and total dissolved solids (TDS) in the four southern Peruvian river basins during the dry and wet seasons. As expected, only modest changes occurred in temperature from the dry to wet seasons, respectively, from 10.5–22.2° to 10.6–22.3 °C in Chili-Quilca basin (denoted CQB); 22°–23.6 °C in Tambo basin (TB), 16.6–22.7° to 17.5–23.7 °C in Camana-Majes-Colca basin (CMB), 20°–23.3 °C in Ocoña basin (OCB). The water temperature in the region is more influenced by the altitude than the season, with site CQB-1 (10.5°–10.6 °C) located at more than 4000 m, the highest elevation site monitored. However, most sampling locations on the Tambo, Camana-Majes-Chivay and Ocoña rivers were within the arid to semi-arid regions of the basins, with warm air and water temperatures occurring during both seasons. In all streams, the pH values over seasons varied from 6.7 to 8.5, with most streams tending to be slightly alkaline (pH > 7). This is consistent with the known presence of carbonate minerals within the southern basins (Alvan et al., 2012). All pH values were within the Peruvian permissible limits (PRL) (MINAM, 2017) during both seasons (5.5–9). Because the electrical conductivity (EC) is used by the portable Hanna water tester to calculate total dissolved solids, both parameters will be described together. Both parameters are an indication of the ionic composition of the water, which for alkaline waters, is generally a reflection of the calcium and magnesium bicarbonate concentrations for freshwaters, but also can result from human activities (domestic and industrial wastewaters and agricultural runoff) (Rusydi, 2018).

During the dry and wet seasons, respectively, the EC values in CQB were 105–4016 and 90–590 μS/cm, in TMB were 1903 and 620 μS/cm, in CMB were 453–995 and 210–730 μS/cm, and in OCB, 327 and 760 μS/cm. In general, the conductivity (i.e., dissolved mineral content) in all basins (except for OCB) increased from the wet to the dry season. These data also reflect some of the differences in the TM composition between these periods and is consistent with the dry season flows containing more groundwater, with the wet season flows containing more snow melt and direct precipitation. As the Ocoña River results indicate,

Table 1
Average water temperatures, pH values, conductivities, and total dissolved solids (TDS) concentrations during the dry and wet seasons, compared to U.S. and Peruvian regulation for drinking water.

			T (°C)		pH		Conductivity (μS)		TDS (mg L^{-1})	
PRL[a]			Δ 3		5.5–9		1600		1000	
EPA[b]			-		6.5–8.5		-		500	
Watershed	Elevation (m)	Sample Site Code	Dry season (n = 3)	Wet season (n = 1)	Dry season (n = 3)	Wet season (n = 1)	Dry season (n = 3)	Wet season (n = 1)	Dry season (n = 3)	Wet season (n = 1)
Chili-Quilca	3875.2	CQB-1	10.5	10.6	7.4	7.8	105	90	50	50
Chili-Quilca	2189.2	CQB-2	14.6	15.2	7.4	7.3	202	130	98	60
Chili-Quilca	2287.2	CQB-3	14.6	15.3	7.6	7.4	201	130	97	60
Chili-Quilca	2116.2	CQB-4	16.6	15.8	8.1	7.4	316	160	160	80
Chili-Quilca	1938.2	CQB-5	17	16.4	7.9	7.4	516	180	258	90
Chili-Quilca	1091.2	CQB-6	22	17.5	8.2	7.8	1175	340	639	180
Chili-Quilca	12.8	CQB-7	22.2	22.3	8.1	6.9	4016	590	2008	310
Tambo	154.2	TB-1	22.6	23.6	8.4	7.4	1903	610	898	320
Tambo	41.8	TB-2	22.1	23.4	8.5	7.1	1814	620	907	320
Camana-Majes-Colca	702.9	CMB-1	22.7	20.4	8.5	7.1	496	210	246	110
Camana-Majes-Colca	697.4	CMB-2	21.2	20.2	8.5	7.2	453	220	227	120
Camana-Majes-Colca	610.8	CMB-3	19.8	19.7	8.3	7.2	475	220	221	110
Camana-Majes-Colca	380.7	CMB-4	19.6	21.1	8.3	6.7	740	290	370	150
Camana-Majes-Colca	1261.6	CMB-5	21.7	20.5	8.3	7.5	995	730	500	380
Camana-Majes-Colca	1278.3	CMB-6	16.6	17.5	8.1	7.1	522	540	261	280
Camana-Majes-Colca	1339.6	CMB-7	16.8	18.6	8.2	7.5	522	580	258	300
Camana-Majes-Colca	15.2	CMB-8	21.5	23.7	8.2	7.2	545	410	271	210
Ocoña	40.2	OCB-1	20.6	23.3	8.3	7.1	327	760	162	400

[a] PRL is the Peruvian Water Quality Standard for drinking purposes and.
[b] EPA is the Drinking Water Standards.

this trend is not universal, as is also the case for another river in East Africa, where ion concentrations increased during the rainy season due to heavy soil erosion (Cosmas, 2011). In the dry season near the mouth of the Quilca (CQB-7) and Tambo Rivers (TMB-1, TMB-2), conductivity values exceeded the PRL standard (Table 1). Consistent with this, these and other downstream sites (CQB-6, CMB-7) exceeded USEPA (USEPA, 2009) maximum permissible values, for total dissolved solids during the dry season.

Furthermore, Kendall's correlation analysis was applied to river water properties to evaluate the relationship among different TM per each season (Figure S-3). In CQB, TDS showed positive correlation (>0.5) with As, B, Ca, K, Li, Mg, Mo, Sc, Si, Sr, and V; EC with As, B, Ca, K, Li, Mg, Sc, Si, Sr and V; and Temperature (T) with B, Ba, Li, Mo, Sr and Ti in the dry season. None of TM analyzed correlated positively or negatively with pH. Meanwhile, during the wet season TDS showed positive correlation with B, Ba, K, Mg, Sc, Sr and V; EC showed strong correlation with all TM, except Mn, Ni, Pb and Ti; and temperature showed positive correlation with B, Ba, K, Mg, Sc, Si, Sr, and V. In CMB, TDS with B, Ca, K, Mg, Sc and Sr, and negatively correlated with Zn; EC positively correlated with B, Ca, K, Mg, Sc, Sr and negatively correlated with Zn during dry season. pH and Temperature showed any correlation with TM. Whilst during the wet season, TDS correlated positively with B, K, Mg, Sc, Sr and V and negatively correlated with Fe; EC positively correlated with B, Ba, K, Mg, Sc, Sr, Si and V and negatively correlated with Fe; temperature only correlated negatively with Si. However, pH did not show any strong (>0.5) correlation with the TM. In TMB, pH correlated positively with Al, As, Ca, Fe, K, Mo, P and Sc and negatively correlated with Sc, Si, T and V; EC correlated positively with As, B, Ba, Fe, Li, Sr and negatively correlated with Se, Si, Ti and V; temperature positively correlated with As, B, Ba, Fe, Li and Sr; meanwhile negatively correlated with Se, Si, Ti, and V during the dry season. The data from TMB during the wet season and OCB in both seasons was not sufficient to be statistically correlated.

The mean values for the TDS were higher in the dry season than in the rainy season in the southern basins (Table 1). The lower values of this parameter and the lower number of cations and anions that positively correlated with TDS in the wet season (SI, Figure S-3) suggest that the runoff water only contributes to its dilution in the rainy season. The average pH values show lower values during the wet season; however, did not show a strong correlation with TM in both seasons. These results suggest that pH may slightly reduce in rainy season due to anthropogenic activities and its runoff interaction (mining activity, agriculture, wastewater inputs, etc.). The average EC values generally are higher during the dry season; however, did show strong correlation with TM during both seasons. These outcomes suggest that hydrological regulated basins (dams) may influence in the higher EC values during the dry season because of the re-suspension on sediment–water interface and TM enrichment; and subsequently its decrease with an increase in rainfall (Vukovic et al., 2014).

3.2. Trace metal concentrations

The average dissolved and total TM concentrations in the four river basins at the 18 sampling sites during each season are presented in Table 2, whereas minimum and maximum values are provided in the SI, Tables S–3. Fourteen of the TM are regulated by the Peruvian government, with the maximum permissible limit (PRL) given in Table 2, along with data on an additional 22 TM that currently are not regulated, with these values given to provide a more comprehensive profile. The dry and wet season flow data are presented in Table 3. Minimum and maximum concentrations of dissolved and total metals (regulated and unregulated) in the dry and wet seasons are reported on in the SI, Tables S–3. Several noteworthy seasonal differences in TM concentrations were found, indicating flow plays a key role in defining TM concentration.

Concentrations of dissolved and total metals were compared to the National Environmental Quality Standard from Peru (PRL) and USEPA (USRL) National Recommended Water Quality Criteria. Comparing the measured concentrations of soluble metals against the regulated standards (PRL and USRL), even the mean values for B (TB), P (CQB) and As (CQB, TB, CMB) exceeded the PRL for drinking water during the dry season, whereas the mean Pb concentration exceeded the limit during the wet season in the Chili-Quilca basin. The average concentration of Mn was found above the USRL during the wet season in the same basin. Obviously, the total metal concentrations were higher than the dissolved concentrations in both seasons. Surprisingly, the unregulated metals of strontium and lithium were detected at medium to high concentrations in dissolved and total forms. The spatial-temporal variations of mean regulated (Fig. 2) and unregulated (SI, Figure S-4) TM is provided from upstream to downstream in all basins.

The *Chili-Quilca Basin* (CQB) has a total drainage area of 13,817 km^2 and is comprised of the Chili-Vítor-Quilca main-stem, and the Siguas River sub-basin. Water flow is impacted by the Pillones (reservoir volume = 76,000 m^3), El Frayle (127,000 m^3) and Aguada Blanca (30,400 m^3) dams, located in the headwaters of the basin. While the Siguas River flows into the Vitor River, forming the Quilca River, administratively, ANA has designated it as part of the Colca-Chivay-Siguas administrative unit due to the extensive water project that has diverted a major portion of the Colca River through tunnels in the mountains to Pitay, where the diverted water enters the Siguas River. This diversion has allowed expansion of the Majes Irrigation District below Pitay (which despite its name, is not irrigated by the Majes River). Hence, the Siguas sub-basin will be discussed as part of the Colca-Majes-Camana Basin.

In the CQB, seven sites were monitored. Sites CQB-1 to CQB-5 were on the Chili river, whereas sites CQB-6 and CQB-7 were downstream on the Vitor and Quilca rivers, respectively (Fig. 1 and Figure S-1). Site CQB-1 is located at the head of the basin, where the population density is very low, and where raising alpaca, llama, and vicuña livestock is the main economy activity. Yet, site CQB-1 is also close to one of the main highways linking Arequipa to the other major southern cities of Cusco and Puno, and therefore is heavily transited by heavy commercial trucks. At this site during the dry season, the geogenic TM arsenic (21 μg L^{-1}) exceeded the PRL, and boron had higher concentration (212 μg L^{-1}) compared to the wet season. The head of this basin is dominated by the presence of several volcanos (e.g., Misti and Chachani), which may explain the high arsenic concentration. Manganese was detected at 50 μg L^{-1} (USEPA maximum limit). While manganese might occur from natural sources, it may also be released to the environment through the use of MMT as a gasoline additive (Lynam et al., 1990). During the wet season, the geogenic TM of Fe (630 μg L^{-1}) and Al (1265 μg L^{-1}) were measured at concentrations above the PRL. It is likely that Fe and Al are leached from upland soils during high rainfall. The associated drop in pH during high rainfall may contribute to the leaching of these TM from clay minerals (Gozzard et al., 2011). In contrast to the dry season, arsenic was detected below the LOQ. Mn deserves some attention as the concentration during the wet season increased to 260 μg L^{-1}, exceeding the USRL.

Sites CQB-2 and -3 are located within the city of Arequipa, the second largest city of Peru, with a population of 990,000 and with several industrial (cement, steal, tannery) and mining (copper, molybdenum, and borates) operations. The region around Arequipa is considered the main minerals producing area of Peru (Ministerio de Enegia y Minas, 2019). In the dry season, arsenic (19 μg L^{-1}) was the only TM detected above the PRL. Manganese was detected at 59 μg L^{-1} surpassing the USRL. In the wet season, aluminum (1532 μg L^{-1}) and iron (1473 μg L^{-1}) were detected above the PRL, and manganese had its highest concentration at 182 μg L^{-1}, exceeding the USRL. Sites CQB-4 and -5 are located near a major mine, especially site CQB-5, which is below the Cerro Verde mine near Arequipa and La Enlozada Wastewater Treatment Plant (WWTP). Water collected at these two sites have similar TM profiles. During the dry season at sites CQB-4 and -5, arsenic was detected at 21 and 20 μg L^{-1}, respectively, exceeding the PRL. However, water from the further downstream site (CQB-5) contained many suspected industrial and

Table 2
Average values and standard deviations (SD) of dissolved and total metal concentrations (μg L^{-1}) in the dry and wet seasons.

ChIli-Quilca Basin (CQB)

Pollutant	Maximum Limit Permissible		Dissolved Metals				Total Metals			
			Regulated				Regulated			
			Dry season ($n = 21$)		Wet season ($n = 7$)		Dry season ($n = 21$)		Wet season ($n = 7$)	
	PRL[a]	USRL[b]	Mean	SD	Mean	SD	Mean	SD	Mean	SD
Al	900	–	65.3	132.9	<LOQ	–	207.9	221.8	1565	311.9
As	10	10.0	16.3	7.2	<LOQ	–	19.9	8.4	12.8	6.2
B	2400	–	1019	1331	158.4	123.3	1072	1416	206.2	135.2
Ba	700	2000	33.8	14.7	28.9	10.5	42.3	15.3	112.0	54.8
Cd	3	5.0	0.4	0.1	<LOQ	–	<IDL	–	<LOQ	–
Cr	50	100.0	2.0	0.6	<IDL	–	1.9	0.9	1.6	0.6
Cu	2000	1300	10.9	9.1	<IDL	–	4.8	2.7	16.7	9.6
Fe	300	300.0	10.0	14.0	6.4	2.4	203.7	173.6	1582.4	241.4
Mn	400	50.0	1.8	1.2	109.9	46.8	62.5	26.7	230.0	91.0
Mo	70	–	7.2	4.4	<LOQ	–	8.1	4.5	<LOQ	–
Ni	70	700.0	<LOQ	–	2.1	0.7	2.1	0.9	3.8	1.4
P	100	–	287.6	422.0	<IDL	–	294.0	475.1	810.6	399.7
Pb	10	15.0	<LOQ	–	162.9	62.1	<LOQ	–	8.9	2.1
Zn	3000	5000	3.0	1.9	<IDL	–	10.2	6.9	6.0	2.0
			Unregulated				**Unregulated**			
Ca	–	–	74,409	137,101	N.R	–	74,210	135,825	N.R	–
Co	–	–	<IDL	–	<IDL	–	2.2	0.5	2.5	1.6
Gd	–	–	<IDL	–	<IDL	–	<LOQ	–	3.2	1.2
Ge	–	–	7.0	2.5	<IDL	–	8.3	3.5	<IDL	–
K	–	–	8079	9872	2664	1424	7060	9568	3373	1598
Li	–	–	76.0	81.9	<IDL	–	80.1	86.7	N.R	–
Mg	–	–	15,321	24,119	4610	2815	15,297	24,079	4858	3161
Nd	–	–	7.5	1.6	<IDL	–	8.4	2.6	N.R	–
Pd	–	–	10.3	2.2	<LOQ	–	4.5	2.3	<IDL	–
Pt	–	–	4.6	2.5	3.3	1.6	3.8	1.7	<LOQ	–
Sc	–	–	31.8	41.7	5.1	4.7	34.8	44.3	7.3	5.6
Si	–	–	10,072	8216	9745	1406	9377	7631	9550	3745
Sr	–	–	328.1	385.4	200.2	160.2	635.0	977.0	216.6	163.4
Ti	–	–	4.4	1.8	7.8	1.6	10.5	9.5	63.0	21.9
V	–	–	13.9	10.6	4.8	2.7	11.0	9.3	10.3	4.8
W	–	–	16.6	3.6	<IDL	–	<LOQ	–	<IDL	–
Yb	–	–	3.3	1.6	<IDL	–	<IDL	–	0.8	0.3
Zr	–	–	<LOQ	–	<IDL	–	<LOQ	–	3.9	1.5

Tambo Basin (TB)

Pollutant	Dissolved Metals				Total Metals			
	Regulated				Regulated			
	Dry season ($n = 6$)		Wet season ($n = 2$)		Dry season ($n = 6$)		Wet season ($n = 2$)	
	Mean	SD	Mean	SD	Mean	SD	Mean	SD
Al	31.8	35.6	69.5	32.3	1147	760.6	2000	0.0
As	209.6	107.9	12.3	4.1	261.0	106.1	80.3	1.6
B	4698	2256	599.5	197.9	5067	2483	699.2	40.8
Ba	47.4	7.7	31.7	8.8	87.9	37.0	424.0	23.1
Cd	<LOQ	–	<LOQ	–	0.7	0.4	1.7	0.1
Cr	<LOQ	–	<IDL	–	3.6	2.1	2.8	0.0
Cu	7.1	2.3	6.3	4.4	48.6	42.7	188.8	7.4
Fe	22.4	18.3	29.2	13.8	1039	804.4	2000	0.0
Mn	1.2	0.5	1.3	0.9	177.2	175.0	1904	135.6
Mo	4.3	1.0	<LOQ	–	4.6	1.0	<LOQ	–
Ni	<LOQ	–	<IDL	–	4.7	2.7	13.5	0.5
P	30.6	30.6	<IDL	–	210.2	226.7	2000	0.0
Pb	<LOQ	–	<LOQ	–	11.2	5.8	47.8	3.2
Zn	2.1	1.2	<IDL	–	59.2	46.5	129.7	2.1
	Unregulated				**Unregulated**			
Au	<IDL	–	<LOQ	–	<LOQ	–	8.7	2.0
Ca	69,493	52,944	N.R	–	74,012	56,217	N.R	N.R
Co	<IDL	–	<IDL	–	5.5	3.9	21.4	1.3
Gd	<LOQ	–	<IDL	–	3.8	2.0	9.3	1.2
Ge	7.4	3.0	<IDL	–	8.7	4.9	<IDL	–
K	13,480	9177	5858	653	12,480	8289	12,237	1340
Li	700.7	258.5	24.1	6.1	706.9	249.5	48.0	5.7
Mg	17,549	12,212	8918	247.2	17,832	12,415	22,012	3114
Nd	<IDL	–	<LOQ	–	9.8	5.1	N.R	–
Pd	<LOQ	–	<LOQ	–	3.4	1.4	<IDL	–
Pt	4.9	2.9	3.1	2.2	3.3	1.7	<IDL	–
Sc	29.8	17.9	17.8	5.0	23.3	19.4	41.8	3.3

(*continued on next page*)

Table 2 (*continued*)

Tambo Basin (TB)

Pollutant	Dissolved Metals				Total Metals			
	Regulated				Regulated			
	Dry season ($n = 6$)		Wet season ($n = 2$)		Dry season ($n = 6$)		Wet season ($n = 2$)	
	Mean	SD	Mean	SD	Mean	SD	Mean	SD
Si	10,760	7701	9843	535	11,026	7245	26,519	3261
Sr	1441	498.7	640.6	3.8	1495	489.3	994.5	128.4
Ti	7.4	1.0	5.0	1.9	60.9	81.9	105.4	7.8
V	<LOQ	–	<LOQ	–	8.1	6.2	36.2	1.9
Yb	<IDL	–	<IDL	–	0.5	0.2	2.5	0.3

Camana-Majes-Colca Basin (CMB)

Pollutant	**Dissolved Metals**				**Total Metals**			
	Regulated				**Regulated**			
	Dry season ($n = 24$)		**Wet season ($n = 8$)**		**Dry season ($n = 24$)**		**Wet season ($n = 8$)**	
	Mean	**SD**	**Mean**	**SD**	**Mean**	**SD**	**Mean**	**SD**
Al	29.4	24.0	111.4	59.1	493.1	646.2	2000	0.0
As	20.0	7.4	<LOQ	–	23.9	8.7	14.2	5.6
B	504.9	210.4	134.4	36.7	552.7	244.2	174.4	34.5
Ba	32.8	11.2	34.7	7.5	50.0	22.2	214.3	84.2
Cd	<LOQ	–	<IDL	–	<LOQ	–	0.7	0.4
Cr	<LOQ	–	<IDL	–	1.3	0.4	2.0	1.0
Cu	3.4	1.8	<LOQ	–	9.1	15.6	23.3	9.2
Fe	13.2	11.8	56.5	52.5	416.7	525.3	1979	58.3
Mn	1.2	0.7	<LOQ	–	61.3	61.4	564.3	292.9
Mo	5.5	3.2	<LOQ	–	5.5	3.1	<LOQ	
Ni	<LOQ	–	<LOQ	–	41.0	48.0	5.2	
P	120.8	223.9	<LOQ	–	179.9	253.6	1101	528.2
Pb	<LOQ	–	<LOQ	–	<LOQ	–	17.7	9.4
Zn	2.2	1.3	<IDL	–	47.2	80.0	35.8	24.6
Unregulated					**Unregulated**			
Au	<IDL	–	<LOQ	–	<LOQ	–	6.0	2.8
Ca	37,683	30,848	N.R	–	38,603	31,645	N.R	N.R
Co	<LOQ	–	<IDL	–	1.5	0.6	5.2	2.1
Gd	<LOQ	–	<IDL	–	<LOQ	–	3.5	1.7
Ge	7.1	2.4	<IDL	–	9.0	3.8	<IDL	–
K	5250	3180	4449	2582	4468	3045	5819	2508
Li	115.5	49.2	<IDL	–	115.8	52.2	N.R	–
Mg	9209	7087	9807	8108	9393	7187	13,923	7685
Nd	<LOQ	–	<LOQ	–	7.7	1.6	N.R	–
Pd	4.4	2.1	<LOQ	–	4.2	2.1	<IDL	–
Pt	4.8	2.8	<LOQ	–	34.8	26.1	<LOQ	–
Sc	19.1	15.6	14.6	7.4	18.4	11.2	37.1	24.5
Si	10,267	7297	11,665	2210	9689	6843	17,023	3718
Sr	495.4	203.7	399.0	184.1	522.3	217.6	487.4	252.5
Ti	6.0	1.2	6.3	1.6	19.2	26.1	91.7	19.9
V	19.6	15.2	5.8	2.7	19.7	13.8	19.8	5.6
W	<LOQ	–	<IDL	–	25.4	5.2	<IDL	–
Yb	<LOQ	–	<IDL	–	<LOQ	–	1.2	0.6

Ocoña Basin (OCB)

Pollutant	Dissolved Metals			Total Metals		
	Regulated			Regulated		
	Dry Season ($n = 3$)		Wet Season	Dry Season ($n = 3$)		Wet Season
	Mean	SD	Single Value	Mean	SD	Single Value
Al	49.1	35.2	41.2	727.9	966.1	2000
As	30.4	9.6	<LOQ	36.2	12.0	29.7
B	540.7	273.4	91.0	619.3	366.9	146.0
Ba	14.5	3.1	34.2	26.7	8.0	397.7
Cd	<IDL	–	<IDL	<IDL	–	1.2
Cr	<IDL	–	<IDL	6.4	3.7	2.8
Cu	5.4	4.3	<LOQ	3.4	1.4	99.1
Fe	16.5	11.3	13.2	485.9	611.1	2000
Mn	1.0	0.2	<LOQ	61.4	22.1	2000
Mo	3.1	1.8	<LOQ	3.1	0.8	<LOQ
Ni	<IDL	–	<IDL	3.2	1.9	9.6
P	39.9	23.1	<IDL	99.2	46.5	2000
Pb	<IDL	–	<IDL	<LOQ	–	38.5
Zn	<LOQ	–	<IDL	12.5	7.2	73.5
Unregulated				**Unregulated**		
Au	<IDL	–	<IDL	<IDL	–	14.5
Ca	23,802	19,647	N.R	24,237	19,488	N.R
Co	<IDL	–	N.R	<LOQ	–	17.9

(*continued on next page*)

Table 2 (*continued*)

Ocoña Basin (OCB)						
Pollutant	Dissolved Metals			Total Metals		
	Regulated			Regulated		
	Dry Season ($n = 3$)		Wet Season	Dry Season ($n = 3$)		Wet Season
	Mean	SD	Single Value	Mean	SD	Single Value
Gd	<LOQ	–	<IDL	<LOQ	–	9.4
K	3123	987.6	5531	2481	626.7	2000
Li	113.2	56.6	<IDL	116.4	56.9	N.R
Mg	3917	1749	5922	4020	1780	2000
Pd	3.3	1.9	<IDL	4.6	2.7	<IDL
Pt	4.8	2.8	3.2	<LOQ	–	<IDL
Sc	10.2	6.5	40.8	12.6	8.0	108.6
Si	10,088	7879	8838	9345	7312	1000
Sr	251.4	112.7	1044	256.0	105.4	1358
Ti	5.0	1.0	4.2	18.5	22.7	111.7
V	8.7	9.0	<LOQ	5.5	0.9	32.3

*Ca, Mg, K, Si and B show results multiplying by dilution factor (30x).
[a] PRL is the Peruvian Water Quality Standard for drinking purposes (Category 1A-2).
[b] EPA is the Drinking Water Standards.

Table 3
Historical seasonal flow rivers variation in southern basins.

Basin	Dry season			Wet season			% variation
	Date	Flow (m^3/S)	Percentile (%)	date	Flow (m^3/S)	Percentile (%)	
CQB	10/13/2019	7.94	53.6	02/17/2020	85.08	99.8	−46.2
TB	10/15/2019	8.35	30.6	2/19/2020	169.82	97.0	−66.4
CMB	10/16/2019	21.36	6.0	2/20/2020	270.27	91.1	−85.1
OCB	10/16/2019	37.17	14.1	2/20/2020	349.85	95.0	−80.9

mine-related TM (Gardner and Carey, 2004; Gozzard et al., 2011) including Zn > Ti > Sc > Ge > Cu > Pd > Pt > Ni > Mo > Cr from 2 to 14 μg L^{-1}. Additionally, at both locations, manganese (59 and 63 μg L^{-1}) and phosphorus (124 and 1332 μg L^{-1}) exceeded the USRL and PRL, respectively.

Nutrients tend to spatially vary depending on land use practices and urban activities with higher phosphorus and reactive nitrogen concentrations generally occurring in areas of urban and agricultural activity (Varol, 2013). The higher phosphorus concentrations in the lower CQB can be explained by the intensively irrigated farms in the Chili Valley (covering about 6900 ha) where some leaching and runoff occurs, even during the dry season. During the wet season, the TM contamination profiles at CQB-4 and 5 were very similar to the dry season; however, Fe (1368 and 1347 μg L^{-1}) and Al (1331 and 1329 μg L^{-1}) concentrations were higher, surpassing the PRL. Manganese (187 and 184 μg L^{-1}) exceeded the USRL at both sites. The increasing concentrations of anthropogenic TM during the wet seasons are well reported in the literature due to erosion of contaminated soil and runoff after atmospheric deposition. This mechanism transports TM from densely populated areas into river systems (Wang et al., 2017; Walaszek et al., 2018).

Sites CQB-6 and 7 are on the Vitor and Quilca rivers, respectively. These sites are at lower altitudes with site CQB-7 very near the Pacific Ocean. Agriculture is the main economic activity at both sites. During the dry season, the suspected geogenic TM, arsenic (24.8 and 17.5 μg L^{-1}), was detected above the PRL at both sites, and boron (3461 μg L^{-1}) was above the PRL at CQB-7. Phosphorus (215 and 274 μg L^{-1}) was detected above the PRL at both sites, and manganese (89 μg L^{-1}) exceed the USRL at site CQB-7. Surprisingly, boron concentration tended to increase at the lower altitudes within the hyper-arid regions, near the coast. At the downstream sites (CQB-6 and 7), a greater number of TM were detected than upstream in the Chili River. The lower basin contained high concentrations of B, Sr, Fe and As. During the wet season, Al (>2000 μg L^{-1}, both sites), Fe (1795 and > 2000 μg L^{-1}) and As (13 μg L^{-1}, both sites) exceeded the PRL; and manganese (189 and 426 μg L^{-1}) exceed the USRL. Phosphorus (711 and 274 μg L^{-1}) was detected above the PRL at both sites. Pb (11 and 13 μg L^{-1}) also surpassed the PRL at CQB-6 and -7.

In summary, the Chili-Quilca basin was impacted by high concentrations of arsenic, boron, manganese, iron, aluminum, phosphorus, and lead. Iron and aluminum concentrations increased dramatically during the rainy season at all sites, surpassing the national regulated criteria (i.e., PRL), whereas arsenic was detected frequently above the PRL during the dry season, and with its concentration decreasing to below the LOQ during the wet season at all sites. Boron followed the same pattern. Manganese was the only TM found above the USRL during both seasons. The river (Chili) at the head of the basin was less contaminated by TM than the middle basin (CQB-2 to 5), as expected due to urban and mining activities associated in and around the city of Arequipa.

The Tambo Basin has a total drainage area of 13,535 km^2 and encompasses three sub-regions of Arequipa (4305 km^2), Moquegua (7858 km^2) and Puno (1371 km^2). The head of the basin is located in the Puno region, the middle-upper part of the basin is the Moquegua region, and lower basin stretches from Arequipa to the coast. The Tambo river is 297 km long and the main tributaries are the Ichuña (65 km), Coralaque-Vizcacha (146 km), Huayrondo (78 km) and Carumas (43 km) rivers. The flow in this basin is partially regulated in the middle-upper section (Moquegua) by the Pasto Grande Dam. The reservoir typically contains 175,000 m^3 water, which is partially released during the dry season for agriculture purposes in the lower Tambo River Valley, which covers 13,000 ha. In addition to irrigation, the water from this river is the source of drinking water for the Islay province, which has 17,614 inhabitants. Additionally, several mining companies operate within the middle and upper parts of the basin. The sites monitored in this study were located in the lower part of the basin (Fig. 1).

Comparing the measured soluble fraction TM concentrations against both PRL and USRL maximum permissible limits (SI, Tables S–3), shows that both B and As exceeded the PRL during the dry season, whereas, only As was detected above the PRL during the wet season. With regards

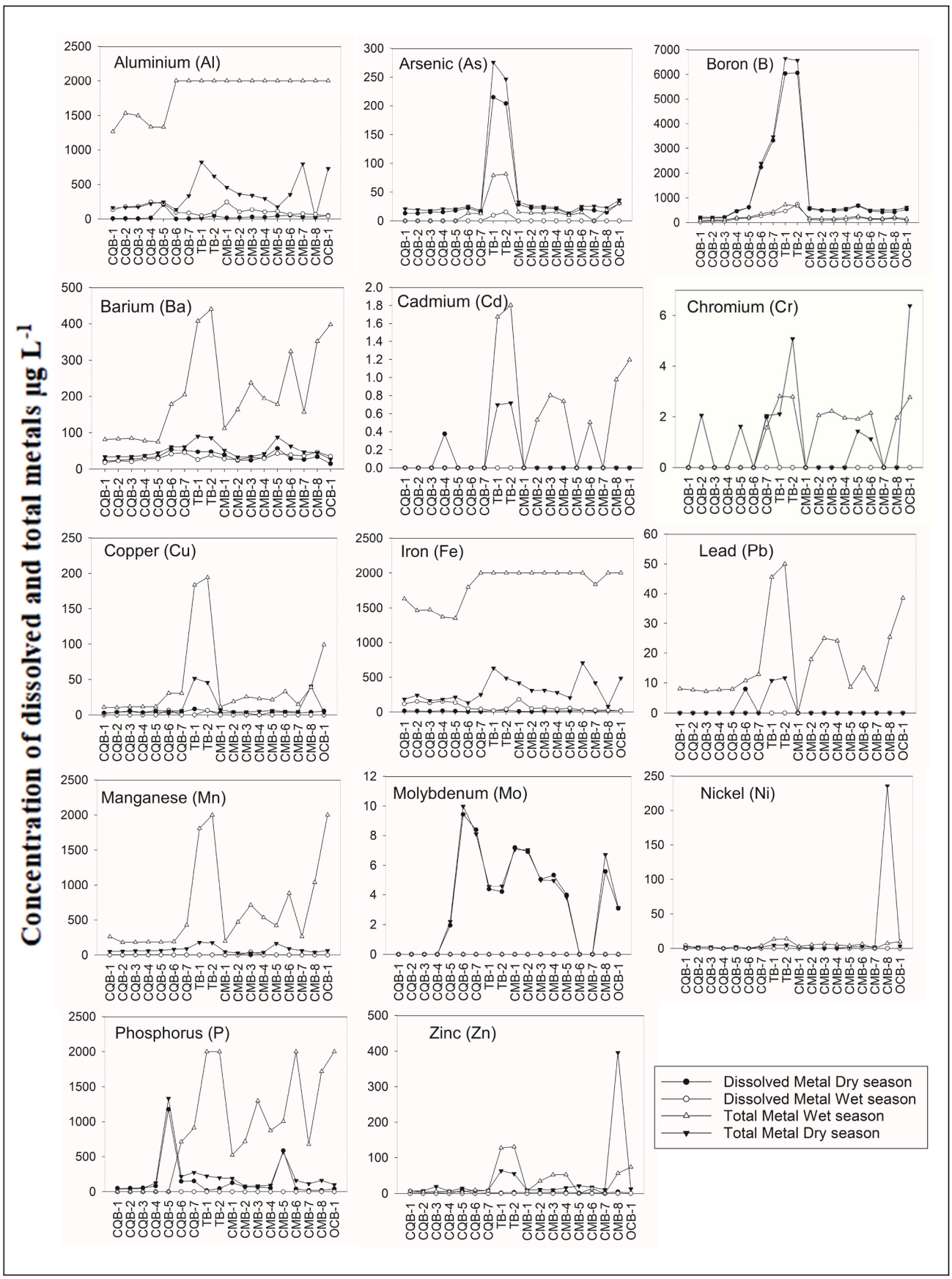

Fig. 2. Spatiotemporal variations in concentrations of dissolved and total metal regulated at Arequipa's basins, Chili-Quilca (CQ), Tambo (TM), Camana-Majes (CM) and Ocoña (OC) basins. The spatial river code assigned is organized from head (e.g., CQB-1) to mouth of basin (CQB-7). Symbols represent total and dissolved metal seasonal variation.

to total recoverable metals, the number of TM which surpassed the PRL was higher in both seasons. During the wet season, B, Al, Fe, P, Mn, As and Pb exceeded their limit, whereas during the wet season, Al, Fe, P, Mn, As and Pb surpassed the PRL. It is evident that during the wet season, dilution of some mineral bearing elements occurred, such as boron, detected at 728 μg L^{-1}, below the PRL of 2400 μg L^{-1}. The most noteworthy concentrations of unregulated dissolved and total metals detected during both seasons were strontium and lithium (SI, Tables S–3).

Sites TB-1 and TB-2 are located near the mouth of the Tambo River. Obviously, dissolved metal concentrations were lower than total concentrations, however seasonal variations in both were consistent. Due to the proximity of these two sites, the measured concentrations are quite similar (Fig. 2). During the dry season, the (suspected) geogenic TM that surpassed the PRL at both sites were Boron (6641 and 6559 μg L^{-1}), Fe (630 and 486 μg L^{-1}), and As (275 and 247 μg L^{-1}). TM and metalloids of suspected anthropogenic origin, including P (223 and 197 μg L^{-1}), Mn (1808 and 175 μg L^{-1}), and Pb (45 and 11 μg L^{-1}), also exceeded the PRL. During the wet season, concentration profiles varied remarkably, indicating an increase in several geogenic and anthropogenic TM, with elements which exceeded the Peruvian water quality threshold at both sites being Fe (>2000 μg L^{-1}), Al (>2000 μg L^{-1}), As (79 and 81 μg L^{-1}), P (>2000 μg L^{-1}), Mn (1808 and >2000 μg L^{-1}) and Pb (45 and 50 μg L^{-1}).

In general, the Tambo basin was found to be highly impacted by boron, arsenic, iron, aluminum, manganese, phosphorus, and lead, as these pollutants often surpassed the PRL in both seasons. Unlike the Chili-Quilca basin, where the highest arsenic concentration was detected at 24 μg L^{-1} and was below the LOQ at the head of the basin, the highest concentration of arsenic in the Tambo basin was detected at 275 μg L^{-1} during the dry season and at 79 μg L^{-1} during the wet season. Thus, the arsenic concentration in the Tambo basin was about ten times greater than in the Chili-Quilca, and the wet season river flow (169.8 m^3/s) was insufficient to dilute this element to acceptable levels. Boron was detected in the Tambo River at the highest concentration found in this study (up to 7461 μg L^{-1}) during the dry period, but diluted to acceptable values during the wet season. The volcanic cordillera region of the Southern Andes and the hyper-arid coastal region of South America (i.e., the Atacama Desert) and have been well reported as natural rich source of boron and arsenic. For example, As was reported in hot springs regions to vary between 3 and 9500 μg L^{-1}, with a maximum concentration of As found near San Antonio de Los Cobres (Argentinian Andes), with high concentrations also found in several north-central rivers of Chile (Pizarro et al., 2010; Hudson-Edwards and Archer, 2012). Also, Boron has been detected at remarkably high concentrations in rivers, and in groundwater and tap water samples from Argentina (4800–6000 μg L^{-1}), Bolivia (507–4359 μg L^{-1}), and Chile (220–11,300 μg L^{-1}). Previously in the Tambo basin, As and B were reported at 15 and 3850 μg L^{-1}, respectively, in city tap water at Mollendo, Peru (Vera, 2017). These previous reports are in good agreement with the findings in this study. In addition, the concentrations of aluminum, iron, lead, and phosphorus tended to increase significantly during the wet season, surpassing the national regulated values. However, all were detected above the PRL during the dry season as well, with the exception of aluminum. From the dry to wet season, the concentrations of P and Mn increased by approximately ten times; Pb by four times, and Fe by three times. During both seasons, the concentrations of suspect anthropogenic TM (i.e., Zn, Cu, Pb, and Nd) generally were greater than in the Chili-Quilca basin. Intensive legal and illegal mining activities, and water release from the Pasto Grande Dam, are two important features at the head of the basin that may play an important role in influencing the concentration and mass flux of geogenic TM from the head to the mouth of the basin during the dry season, when rainfall and runoff are less significant direct mechanisms causing TM transport to the river. For instance, a previous study reported that at high flow rates through the Danube Dam, located on the Danube River in Europe, fluvial erosion took place in the river and caused re-suspension and downstream transport of Cu, Zn, Pb and Cd on suspended sediments (Vukovic et al., 2014).

The *Camana-Majes-Colca (Colca-Majes-Camana) basin* covers a drainage area of 17,152 km^2. The Colca River is 388 km long and has its origin in the western Andes flank at 4886 m. Upper basin rivers include the Chilamayo, Andamayo, and Colca, and the main Colca River stem becomes the Majes River in the mid-basin, and the Camana River in the lower basin. The National Water Authority (ANA) divided this and the adjacent basin into two administrative areas for managing purposes, the Camana-Majes and the Colca-Chivay-Siguas administrative authorities. This is because a large portion of the Colca River is diverted through a canal which often runs through tunnels in the mountains, to the Siguas River located in the adjacent natural hydrologic basin. The flow in the basin is highly regulated by dams at Condoroma (259,000 m^3), El Pañe (99,600 m^3) and Los Españoles (9900 m^3) in the head of the basin. Within the Colca-Chivay-Siguas administrative basin is one of the main irrigation districts of Peru, the Majes-Siguas irrigation district (Stage I), which covers 23,000 ha, located in one of the most hyper-arid regions of the world (Maos, 1985). It is adjacent to the Siguas River, and is an important economic activity for the Arequipa region. It is because of the size of this irrigation district that the water is diverted from the Colca River to the Siguas River, upstream from this irrigation district. In addition, the Majes and Camana River Valleys contain about 8000 and 6400 ha, respectively, and have intensive agricultural activities. Additionally, several mining companies operate in the upper and middle-upper portions of the Camana-Majes-Colca basin.

Eight strategic sites were monitored in the Majes and Camana Valleys and in the Majes irrigation District (Fig. 1 and SI, Figure S-1). Across these eight sites, dissolved metalloids that exceeded the PRL during the dry season were P and As (SI, Tables S–3). During the wet season, all dissolved metals were below the PRL. However, total recoverable metals that exceeded the PRL in the dry and wet seasons were Al, Fe, P and As. With respect to unregulated TM, total and dissolved fractions of strontium and lithium showed the highest concentration in the dry and wet seasons.

Figure 2 and Figure S-4 show the spatiotemporal variation profiles. In the Camana-Majes-Colca basin (denoted CMB), site CMB-1 is located on the Quebrada de los Molles stream; CMB-2, -3 and -4 are located on the Majes River, and CMB-5 is located on the Siguas River, but contains some river water diverted from the Colca River. Sites CMB-6 and -7 are the inflow and outflow from an artificial pond within the Majes Irrigation district which is water that was diverted from the Siguas River at Pitay. Site CMB-8 is located at several kilometers upstream from the confluence of the Camana River with the Pacific Ocean.

During the dry season, water from the Quebrada del Castillo stream (CMB-1), contained arsenic (33 μg L^{-1}) and Fe (417 μg L^{-1}) at concentrations surpassed the national water quality threshold. Additionally, phosphorus (189 μg L^{-1}) was detected above the PRL. During the wet season, Al (>2000 μg L^{-1}), Fe (>2000 μg L^{-1}), As (15 μg L^{-1}), and P (522 μg L^{-1}) exceeded the PRL, and Mn (197 μg L^{-1}) was above the URSL.

Sites CMB-2, -3 and -4 are near the towns of Acoy, Aplao and Corire, respectively, all in the Majes River valley, and hence the TM concentration patterns were quite similar during both seasons. In the dry season, Fe and As were found above the PRL at all three sites. During the wet season, the suspected geogenic TM and metalloids of Al, Fe, As, P, Mn and Pb were detected above PRL at all three locations.

Sites CMB-5, -6 and -7 are located on the Siguas River at Pedregal (Highway 1 S bridge), and at the inflow and outflow of a retention pond located in Pedregal, respectively. During the dry season, only As (13 μg L^{-1}) surpassed the PRL at these locations. However, in the wet season, Al (>2000 μg L^{-1}), Fe (>2000 μg L^{-1}), P (1004 μg L^{-1}) and Mn (419 μg L^{-1}) surpassed the PRL. The retention pond associated with sites CMB-6 and -7 serve mainly as a water storage pond, but also to reduce the suspended solids concentration prior to irrigation. Settling of solids also

may reduce TM concentrations. Indeed, during the dry season, the inflow (CMB-6) water had higher concentrations of Fe (706 μg L^{-1}) compared to the outflow (CMB-7) at 419 μg L^{-1} Fe. The concentration of As (25 μg L^{-1}) did not change from the inflow to outflow of the retention pond. Further, P (159 μg L^{-1}) and Mn (89 μg L^{-1}) were above the PRL and USRL, respectively, in the inflow, whereas the outflow contained less P (112 μg L^{-1}) and Mn (61 μg L^{-1}), suggesting some settling of these elements occurred in the pond.

During the wet season, Al was detected at >2000 μg L^{-1} in the inflow and the outflow, surpassing the PRL. Iron decreased from >2000 in the inflow to 1835 μg L^{-1} in the outflow, but surpassed the PRL in both cases. Arsenic was detected at 14 μg L^{-1} in the inflow and was below the LOQ in the outflow. Phosphorus (>2000 μg L^{-1}), Mn (878 μg L^{-1}) and Pb (15 μg L^{-1}) were found above the PRL in the inflow, with lower concentrations of P (676 μg L^{-1}) and Mn (263 μg L^{-1}) in the outflow, yet at higher concentrations than during the dry season.

At Site CMB-8, near the confluence of the Camana River with the Pacific Ocean, As (22 μg L^{-1}) was the only suspected geogenic TM or metalloid that exceed the PRL during the dry season. For suspected anthropogenic elements, Ni (236 μg L^{-1}) and P (160 μg L^{-1}) were found above the PRL. During the wet season, Al (>2000 μg L^{-1}), Fe (>2000 μg L^{-1}), As (18 μg L^{-1}), P (1718 μg L^{-1}), Mn (1037 μg L^{-1}), and Pb (25 μg L^{-1}) were detected above the PRL.

In summary, the TM and metalloids of concern in the river waters of the Camana-Majes-Colca basin were mainly As, Fe, Pb, Ni, Mn, and P. Each of these elements showed a consistent seasonal pattern across the sampling sites. For instance, in the dry season, As and Fe were detected at high concentrations, surpassing the national regulatory limits at all sampling sites. In the wet season, Al, As, Mn, P and Pb were detected above the PRL and USRL. The number of the suspected anthropogenic TM was greater at the sampling site near the ocean, with higher concentrations during the wet season. During the wet season, transport of elements of concern occurs from mid- and upper-basin sites, where mining activity occurs, to the lower basin river. This occurs in the Tambo and Chili-Quilca basins as well, as the economy activities are quite similar in these southern Peruvian river basins. In the CMB, the maximum concentration of B (689 μg L^{-1} at CMB-5) was detected during the dry season in Siguas River water. Yet, this concentration was lower than concentrations measured in the Tambo and Quilca rivers. In the Majes River in the Western adjacent natural hydrologic basin, P was consistently detected at high concentrations during the wet season. Because agriculture is a dominant economy activity in the Majes River valley, the high phosphorous concentrations are likely associated with this activity.

The Ocoña Basin covers a drainage area of 15,334 km^2. The Ocoña river is 238 km long, and the main tributaries are the Maran (82 km), Cotahuasi (158 km) and Chichas-Armas (90 km) rivers. Unlike the Chili-Quilca, Camana-Colca-Siguas, and Tambo basins, the rivers in the Ocoña basin are not artificially regulated by dams. However, the Ocoña basin is influenced by continuous melting of glaciers associated with the Coropuna Volcano. Agriculture and mining are the most important economy activities within this basin, with extensive "informal" mining activities (Nieto, 2019) (i.e., safety reasons) preventing us from sampling anywhere upstream of the town of Ocoña near the river's confluence with the Pacific Ocean.

At the sampling site near the mouth of the river (OCB-1), the number of total recoverable metal and metalloid elements that surpassed the PRL was great. For instance, Al, Fe, P, Mn, and As were detected above the PRL in the dry season, and Al, Fe, P, and As were above the PRL in the wet season. Based on concentration, the most relevant unregulated TM detected were Sr and Li, and were detected in both seasons. Comparing the measured dissolved metal concentrations against the PRL, only arsenic (36 μg L^{-1}) exceed the regulatory limit (SI, Tables S–3), and only during the dry season.

3.3. Temporal variations in southwestern Andes rivers

The Chili-Quilca, Tambo, Camana-Majes-Colca, and Ocoña Basins have many of the same features, with the upper to middle basins relying on mining and agriculture as the dominant economic activities, and the lower basins dominated by productive river valleys, separated by vast arid regions. River water in all the basins is affected by volcanic and other geothermal features, especially in the case of the upper Tambo River Basin.

The flow of each river at each sampling point was classified as high or low by comparing its value during the sampling event to the flow measurements over the last fifty years at each point where data were available, normalizing the data to a scale of 0–100 (i.e., percentile) (Table 3). Figure S-6 displays the changes in flow from the dry to wet season in the basins studied. The flow data were obtained from SENAMHI (National Meteorological Service) and AUTODEMA (Autonomous Authority of Majes) for six hydrological stations in the basins studied (Fig. 1 and Figure S-1). For the stream flow values during sampling events during the wet season (February 2020), the water flow in all four basins was above the 90th percentile, indicating these samples were indeed collected near the peak flows within each basin. Samples collected during the "dry" season (during the October 2019 sampling campaigns) were collected when the stream flows ranged from the 6th to 54th percentile of the historical values.

Our first approach to establishing the parameters associated with seasonal variations was to use the Spearman non-parametric correlation coefficient. These bivariate results showed that among the 38 TM and metalloids investigated, the concentrations of nineteen of the elements exhibited significant correlation (positive or negative) with season. Al (0.887), As (−0.579), Au (0.733), B (−0.674), Ba (0.786), Cd (0.741), Co (0.694), Cu (0.626), Fe (0.879), Gd (0.580), Ge (−0.570), Li (−0.926), Mn (0.866), Ni (0.548), Pb (0.806), Pd (−0.688), Ti (0.813), Yb (0.931) and Zr (0.987) displayed significant correlations with season (SI, Tables S–4). The remaining elements showed no correlation with season. A boxplot was constructed to summarize the total metal concentrations distribution per season for the four basins studied (Fig. 3 and S-5). The outliers mainly included TM concentrations measured in Tambo River water, which contained high concentrations of B, As, Ba, Cu, Pd, Mn, Co, Ge, and Li.

Furthermore, paired sample student t-test was executed to compare if the means of the two seasonal TM concentration have significant variation ($P \leq 0.05$). Tables 4 and S–5 shows that for most (twenty TM = t-student and nineteen TMs = spearman analysis) of the TM their calculated values ($t_{calculated}$) are less than $P \leq 0.05$, which concur with spearman correlation analysis. Additionally, phosphorus correlated with significantly with season through t-student analysis.

Industrial discharges, including mining and agriculture, and municipal wastewater effluents are potential anthropogenic sources of TM and metalloids entering the aquatic environment, whereas surface runoff and atmospheric deposition constitute seasonal sources (Gardner and Carey, 2004). Groundwater discharge to rivers may also constitute a seasonal source, depending on the seasonal contribution to the overall flow and the magnitude of the associated mineral weathering. Indeed, seasonal variations in precipitation, surface runoff, and groundwater discharge substantially impact river flow and the associated concentrations of TM and metalloids in the river water. In this study, the concentrations of 15 TM (Al, Au, Ba, Cd, Co, Cu, Fe, Gd, Mn, Ni, P, Pb, Ti, Yb and Zr) were consistently higher in the Chili-Quilca, Tambo, Ocoña and Camana-Majes-Colca basins during the wet season. Conversely, concentrations of As, B, Ge, Li, and Pd were higher during the dry season sampling events.

Higher wet season TM concentrations have been documented by others (Gundersen and Steinnes, 2001; Yao et al., 2014; Nyantakyi et al., 2019) who postulate that the higher flow rates promote an increase in TM transport because of runoff and desorption. Generally, human activities such as farming, mining, and other urban industry, negatively

Table 4
Paired sample *t*-test for difference in concentration between the wet and dry seasons in southern basins of Peru.

Metals	Pair	Mean (μg L^{-1})	N	Std. Dvtion	t	df	$P <$ 0.05
Al	Dry	355.27	18	238.74	−21.84	17.00	0.00
	Wet	1831.00	18	286.11			
As	Dry	49.40	18	77.33	2.28	17.00	0.04
	Wet	19.71	18	22.80			
Au	Dry	0.00	18	0.00	−5.25	17.00	0.00
	Wet	4.72	18	3.81			
B	Dry	1434.66	18	2048.99	2.71	17.00	0.01
	Wet	243.52	18	186.67			
Ba	Dry	50.29	18	20.29	−5.77	17.00	0.00
	Wet	208.00	18	124.20			
Cd	Dry	0.08	18	0.23	−6.94	17.00	0.00
	Wet	0.62	18	0.49			
Co	Dry	1.14	18	2.06	−4.35	17.00	0.00
	Wet	6.62	18	6.64			
Cu	Dry	11.49	18	15.98	−3.02	17.00	0.01
	Wet	43.32	18	56.81			
Fe	Dry	317.49	18	173.04	−27.95	17.00	0.00
	Wet	1828.43	18	250.62			
Ge	Dry	4.48	18	5.06	3.76	17.00	0.00
	Wet	0.00	18	0.00			
Li	Dry	168.01	18	202.97	3.51	17.00	0.00
	Wet	0.00	18	0.00			
Gd	Dry	0.43	18	1.24	−4.95	17.00	0.00
	Wet	3.31	18	3.16			
Mn	Dry	75.49	18	48.27	−4.05	17.00	0.00
	Wet	662.93	18	638.33			
Ni	Dry	14.82	18	55.14	0.75	17.00	0.47
	Wet	5.19	18	3.66			
P	Dry	223.60	18	302.78	−3.38	17.00	0.00
	Wet	914.66	18	763.93			
Pd	Dry	2.90	18	2.15	5.71	17.00	0.00
	Wet	0.00	18	0.00			
Pb	Dry	1.24	18	3.63	−6.31	17.00	0.00
	Wet	18.11	18	13.92			
Ti	Dry	20.41	18	17.66	−13.85	17.00	0.00
	Wet	83.16	18	25.38			
Yb	Dry	0.03	18	0.12	−6.91	17.00	0.00
	Wet	1.12	18	0.71			
Zr	Dry	0.00	18	0.00	−109.82	17.00	0.00
	Wet	3.41	18	0.13			

impact water quality (Le Pape et al., 2014). Consequently, the wet season urban runoff tends to contribute to TM pollution in surface water bodies (Lavado Casimiro et al., 2012). On the contrary, the current study found higher concentrations of As, B, Ge, Li, and Pd in river water during the dry season. It is likely that the elements (i.e., metalloids, in this case) of most concern are arsenic and boron since these are regulated and consistently exceeded the PR in water samples from several of the sampling locations with the study area.

While arsenic generally was detected above the PRL in samples collected in both seasons, boron generally was at permissible limits (below the PRL) in the wet season samples. There are few studies on the seasonal behavior of arsenic and boron in rivers. Pari-Huaquisto et al. (2020) reported higher As concentration in the dry season (765 μg L^{-1}) and lower concentration in the wet season (331 μg L^{-1}) in Ananea river, a southern basin in Peru. Nguyen et al. (2020) have reported that B and Sr were at higher concentrations in the dry season, relative to the rainy season, but in sediment samples from Saigon River, Vietnam (Nguyen et al., 2020). Hudson-Edwards and Archer (2012) reported on boron concentrations in San Antonio filtered tap water, with the source water ranging from 4.63 to 5.33 mg L^{-1}. The authors pointed out that the water may be improved for drinking and irrigation by dilution with cleaner meteoric waters, or through mineral precipitation, or through the use of commercial filters (Hudson-Edwards and Archer, 2012). Boron mainly occurs in superficial water as non-dissociated boric acid (H_3BO_3), since its pKa is 9.2. Its acidity occurs through abstraction of OH^- from water forming $B(OH)_4^-$, making it a Lewis acid rather than a Brønsted Acid. Other species also may occur, such as tetraborate ($H_4B_4O_9^{2-}$), hence, all oxygenated boron molecules are collectively termed "borates". One of the main sources of boron is saline lakes, whose deposits of boron-containing salts are associated with volcanic and other geothermal activity that occurred as early as the Neogene age in tectonically active regions on plate boundaries with arid climates, such as the Andean range in South America. Peru is among the most important sources of continental borates, with one site (Laguna Salinas, Arequipa) having reserves that exceed 10 million tons of boric anhydride (B_2O_3) (Millas, 2020). Boron is found in stream water because of leaching from the surrounding geological formations and, to a much lesser extent, through wastewater discharges. Boron species generally are not removed by conventional wastewater and drinking-water treatment methods (WHO, 2009).

Arsenic was ubiquitous in study samples, with higher concentrations in the dry season samples than in wet season samples. However, even seasonal variations did not decrease the As concentrations in the wet season to within permissible limits (<10 μg L^{-1}), yet notable dilution was observed (Figs. 2 and 3). For instance, at site TB-1, arsenic was detected at 275 μg L^{-1} in the dry season, and at 79 μg L^{-1} in the wet season. There are few studies on seasonality of As concentrations in superficial riverine waters. Zhang et al. (2020) reported that Arsenic concentrations varied greatly with season in the main stem of a river, with lower As concentrations in the lower reaches of the same river (Zhang et al., 2020). There are numerous reports on As concentrations in wells. For instance, Schaefer et al. (2016) reported that during rainy periods in the Yangtze River Basin, ground water recharge resulted in increased $\delta^{18}O$ (systematic of rain water inputs), which caused Fe(II) and As(III) oxidation, in turn, resulting in a decrease in well water arsenic concentrations (Schaefer et al., 2016). In addition, Buragohain et al. (2010) reported higher Al, Pb, Cd, and As concentration during the dry season, compared to the wet season, in the Dhemaji district of Assam, India. The authors suggested that the main source of arsenic was natural, since the study area was within an alluvial basin with extensive sediment depositions due to surface erosion from the surrounding hills (Buragohain et al., 2010). Therefore, it is possible that arsenic oxidation from As(III) to As(V) occurs in the Peruvian southern basins during the wet weather periods, leading to decreased As concentrations, as it is known that As(V) ($H_2AsO_4^-$ and $HAsO_4^{2-}$) at near neutral pH values are less soluble in the presence of several di- and tri-valent metal cations compared to As(III) (i.e., H_3AsO_3) (Masscheleyn et al., 1991). Alternatively, arsenic from groundwater sources may simply be diluted by high water flows during the dry season. Alkalinity is known to counteract negative effects of TM contamination in aquatic environments as it acts as a buffer (Gundersen and Steinnes, 2001). There was not a significant seasonal correlation with Mg, K, Sr. However, Li and Ba showed a significant positive correlation. Furthermore, it can be observed that K and Mg and pH values were higher in the dry than wet season. Therefore, these parameters would not be generally expected to counteract TM stress during high runoff episodes. However, during the dry season, when continuous flow occurs due to artificially regulation through dams, this may be positive in reducing water acidity in the southern basins.

4. Pollution source identification (multivariate analysis)

Tables 5 and S–6 displays seven principal components extracted for each season based on Eigenvalues, at 86% (dry) and 90% (wet) of the total variance.

For the dry season, the first (PC-1) component (Mg, Ca, Sc, K, Sr, TDS, conductivity) and PC-7 (P) explain 32% and 3% of the variance for this season, respectively. The major components were the alkaline earth metals, TDS, and phosphorus. During the dry season, stream flow in the southern Peruvian basins is highly regulated by discharge from mountain reservoirs, as intensive irrigated agriculture on the arid plains occurs even during this season, which may also contribute to increase

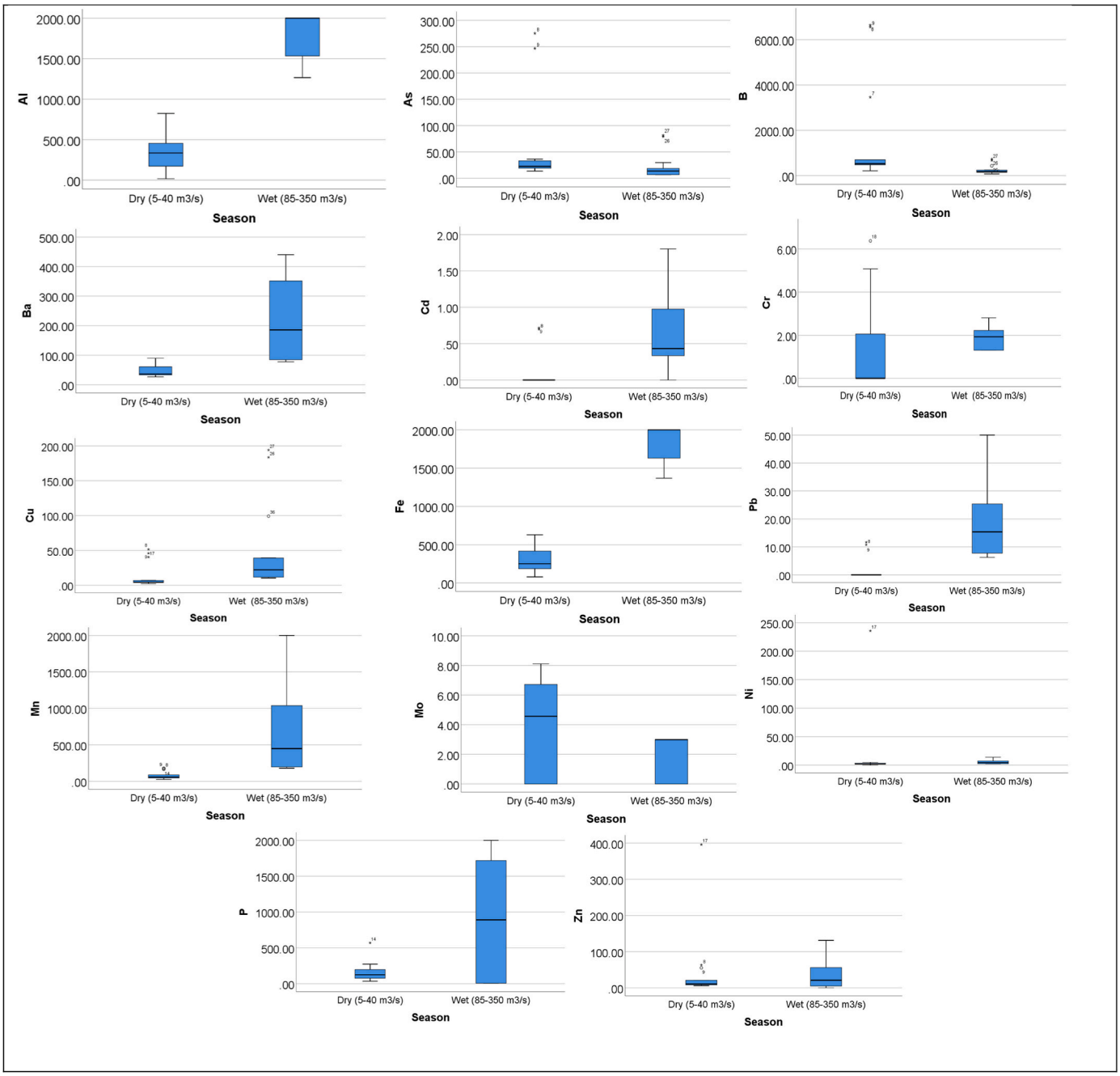

Fig. 3. Boxplot for the total metal (regulated) concentrations (μg L^{-1}) during the dry season and wet Season. The horizontal black lines (inside the boxes) denote the medians of the concentrations. The bottom and top of the box show the first and third quartiles (Q1 and Q3). The individual points with values outside these limits represent outliers. The Y and X-axis represent the concentration level and season, respectively.

solute (including nutrient) concentrations in the rivers (Stets et al., 2014). Components PC-2 (Mn, Ti, Fe, Al, Co, Cr, Nd, Ba), PC-4 (Ni, Pt, Zn), PC-5 (V, Mo, Si), and PC-6 (pH and Temperature), accounted for 21%, 7%, 5%, and 4% of the variance, respectively. These components may include contributions from some anthropogenic sources, including heavy industries, tanneries, mines, and WWTPs (Gardner and Carey, 2004). Note that pH and temperature are variables that are strongly associated. Furthermore, elements in PC-3 (As, Li, B, Pb), which accounts for 11% of the variance, are heavily linked to the natural geochemical composition of the western Andean soils, as arsenic, boron, and lithium have been well documented to occur in several basins from Chile, Argentina, and through Bolivia (Standen et al., 2018). In the headwaters of the study area, the Arequipa and Barosso volcanic groups are part of the landscape. These two volcanic groups have been reported to melt Precambrian granulite gneiss, which has a high lead content (Tilton and Barreiro, 1980). Therefore, the elements in PC-3 are all assumed to be of geogenic origin (Tilton and Barreiro, 1980).

For the wet season samples, PC-1 (Lu, Zn, Cu, Co, As, Pb, Mn, Cd, Ni, Gd, Yb, Ba, P, V, Au), PC-5 (Sc, Sr, Mo), PC-6 (Nd, Pd), and PC-7 (pH and temperature) accounted for 54%, 4%, 3%, and 2% of the variance, respectively. The TM and metalloids in these components likely come from many sources (e.g., soil-erosion, volcanic activity, urban and agricultural runoff, municipal and industrial wastewater discharges). During the wet season, Pb, which presumably occurs through volcanic activity, was detected in several basins above the PRL at concentrations as high as 50 μg L^{-1} (Tambo basin) (Zehetner and Miller, 2006). PC-2

Table 5
Assessment of metal pollution source during the dry and wet seasons, in bold high loading factor (>0.6).

Principal Components (Dry season)							
Contaminant	PC-1	PC-2	PC-3	PC-4	PC-5	PC-6	PC-7
Mg	**0.969**	0.106			0.114		
Ca	**0.957**				0.248		
Sc	**0.952**				0.244		
K	**0.911**		0.317			0.107	0.102
Sr	**0.793**	0.267	0.351		0.224		
TDS	**0.715**	−0.440	0.284			0.203	
EC	**0.692**	−0.444	0.300		−0.127	0.221	
Mn		**0.898**	0.184				0.187
Ti		**0.868**	0.391				0.152
Fe	−0.110	**0.860**				−0.103	
Al	−0.112	**0.820**	0.108	−0.112			
Co		**0.695**	0.516	0.237			
Cr	0.196	**0.676**			−0.219	0.305	
Nd	0.184	**0.663**	0.205		−0.204		−0.388
Ba	0.412	**0.640**	0.376		0.127		0.347
As		0.307	**0.919**				
Li	0.282	0.220	**0.888**			0.107	
B	0.486	0.247	**0.809**				
Pb		0.555	**0.608**		0.155		
Cu		0.549	0.572	0.550			
Ni				**0.990**			
Pt		−0.103		**0.987**			
Zn		0.104		**0.986**			
V	0.128	−0.147	−0.152	0.116	**0.908**		
Mo	0.523		0.111	0.137	**0.788**	0.139	
Si	0.526		0.138	−0.109	**0.725**	0.151	0.259
pH	0.118					**0.834**	0.175
T °C	0.125		0.249	0.105	0.233	**0.793**	−0.191
P		0.151	−0.165				**0.757**
Pd	−0.452		−0.273				−0.576
Principal Components (Wet season)							
Contaminant	Component						
	PC-1	PC-2	PC-3	PC-4	PC-5	PC-6	PC-7
Lu	**0.942**				0.141		0.105
Zn	**0.935**	0.191	0.190				
Cu	**0.934**	0.137	0.264				
Co	**0.912**	0.324	0.159		0.160		
As	**0.900**	0.112	0.338	0.120			
Pb	**0.887**	0.300	0.156		0.148	0.152	
Mn	**0.883**	0.350	0.103		0.262		
Cd	**0.876**	0.382	0.177				
Ni	**0.846**	0.400	0.218	−0.135			
Gd	**0.838**	0.398	0.145		0.278		
Yb	**0.825**	0.474		−0.138	0.157		
Ba	**0.743**	0.510	0.190		0.320	0.103	
P	**0.683**	0.500	0.220	−0.103	0.389		
V	**0.665**	0.529	0.342	−0.102	0.327	0.133	
Au	**0.640**	0.332			0.186	−0.200	0.158
Zr	0.303	**0.889**		−0.137		0.182	−0.169
Fe	0.370	**0.877**		−0.153		0.157	−0.142
Al	0.362	**0.875**	0.100	−0.153		0.161	−0.114
Ti	0.412	**0.822**	0.201	−0.132	0.165	0.129	
Cr	0.593	**0.744**	0.113	−0.129	0.124	0.140	
Pt	−0.373	**−0.655**	−0.142		0.118	−0.199	−0.179
Mg	0.162	0.157	**0.868**		0.326	0.117	0.102
Si	0.351	0.215	**0.845**				
K	0.340	0.111	**0.840**	0.194	0.206		
EC	−0.160	−0.356		**0.802**	0.114	0.164	0.156
TDS	−0.164	−0.349		**0.801**	0.120	0.184	0.145
Li				**0.767**		−0.482	
B	0.487		0.365	**0.696**			
Sc	0.445	0.280			**0.808**		
Sr	0.502		0.252	0.179	**0.744**		0.134
Mo	0.122	−0.104	0.342	0.307	**0.697**	0.107	
Nd		−0.398	−0.130			**−0.775**	
Pd		−0.440	−0.183		−0.242	**−0.694**	0.110
pH			0.119		0.185		**0.841**
T °C	0.197	−0.175		0.205			**0.826**

(Zr, Fe, Al, Ti, Cr, Pt), PC-3 (Mg, Si, K) and PC-4 (conductivity, TDS, Li, B) explained 13%, 7%, and 4% of the variance, respectively. Aluminum and iron routinely were detected at high concentrations during the wet season. These elements (Al, Fe) are associated with leaching from peat-rich uplands, with leaching rates affected by redox conditions. Leaching of humic and fulvic acids can lead to lower pH values, which in turn facilitates leaching of aluminum from clay minerals (Gozzard et al., 2011).

Hierarchical cluster dendrograms analysis (Fig. 4) show similar trend as PCA analysis. A group of EC, TDS, Sc, Ca, K, Mg, Sr, V, Mo, T °C, pH, Si, Ba, Pd and P was obtained in one cluster (A); Li, B, As, Al, Fe, Mn, Ti, and Cu in second cluster (B) whereas Zn, Pt and Ni in a third cluster (C). These results backup PCA elucidation source from the dry season, especially the subgroup of Li, B and As (geogenic origin) and Zn, Pt and Ni (anthropogenic origin), which are clearly linked to geogenic and anthropogenic sources, respectively. Therefore, during the dry season the natural mineral background of the southern Andes and mining activity in convergence with the natural erosion and sediment–water resuspension at high flow rate from reservoirs ubicated in the head of basins influence in the presence of these contaminants. Meanwhile, during the wet season, a group of Al, Fe, Zr, Ti, Ni, Cd, Yb, Ba, V, Pb, Au, Mn, Co, Gd, P, As, Cu and Zn was obtained in one cluster (A), which may have a geogenic/anthropogenic source as clearly can be observed one subgroup dominated by As, Cu and Zn (mining markers) and the remaining TM from a natural background. Meanwhile, T °C, pH, Pt, Sr, Sc, K, Mg, Si, B, Mo, EC, TDS, Pd and Li were associated in second cluster (B), which may be influenced predominantly by geogenic sources as the physical chemical (e.g., pH, EC and T °C) and Ka, Mg and Si were linked in two subgroups. These results concur with the wet season PCA source elucidation. Runoff and its interaction with geogenic and anthropogenic sources may converge to finally influence on the presence of these contaminants in the studied basins (Fig. 4B).

5. Comparison to seasonal TM behavior reports around the world

In order to put the study area into context within the global TM seasonal trends, the data in current study were compared with those in other regions in the world. Compared with other reports on seasonal TM behavior worldwide (Table 6), concentration of Ba, Cr, Cu, Fe, Mn, Ni and Pb followed the same pattern of the present study in China, as these TM concentrations were consistently higher in the wet season (Yao et al., 2014). Furthermore, Pb was reported at higher concentration in the same season in Ghana (Nyantakyi et al., 2019). Meanwhile, arsenic was detected at higher concentration in the dry season in India (Buragohain et al., 2010). In contrast, Cd, Co, Cr, Cu, Fe, Mn, Ni, Pb, Zn, Sr, Al and As, followed the opposite pattern to this study in Pakistan, Ghana, Nigeria, and India (Buragohain et al., 2010; Kumar et al., 2013; Omono et al., 2014; Nyantakyi et al., 2019; Saleem et al., 2019). It is noteworthy that there are scarce studies on TM seasonal studies worldwide. Furthermore, the TM seasonal differences may not only be influenced by the emission of pollutants caused by industrial and mining enterprises in the watersheds, but also be affected by the local geography, natural background and physical–chemical properties in the local environments.

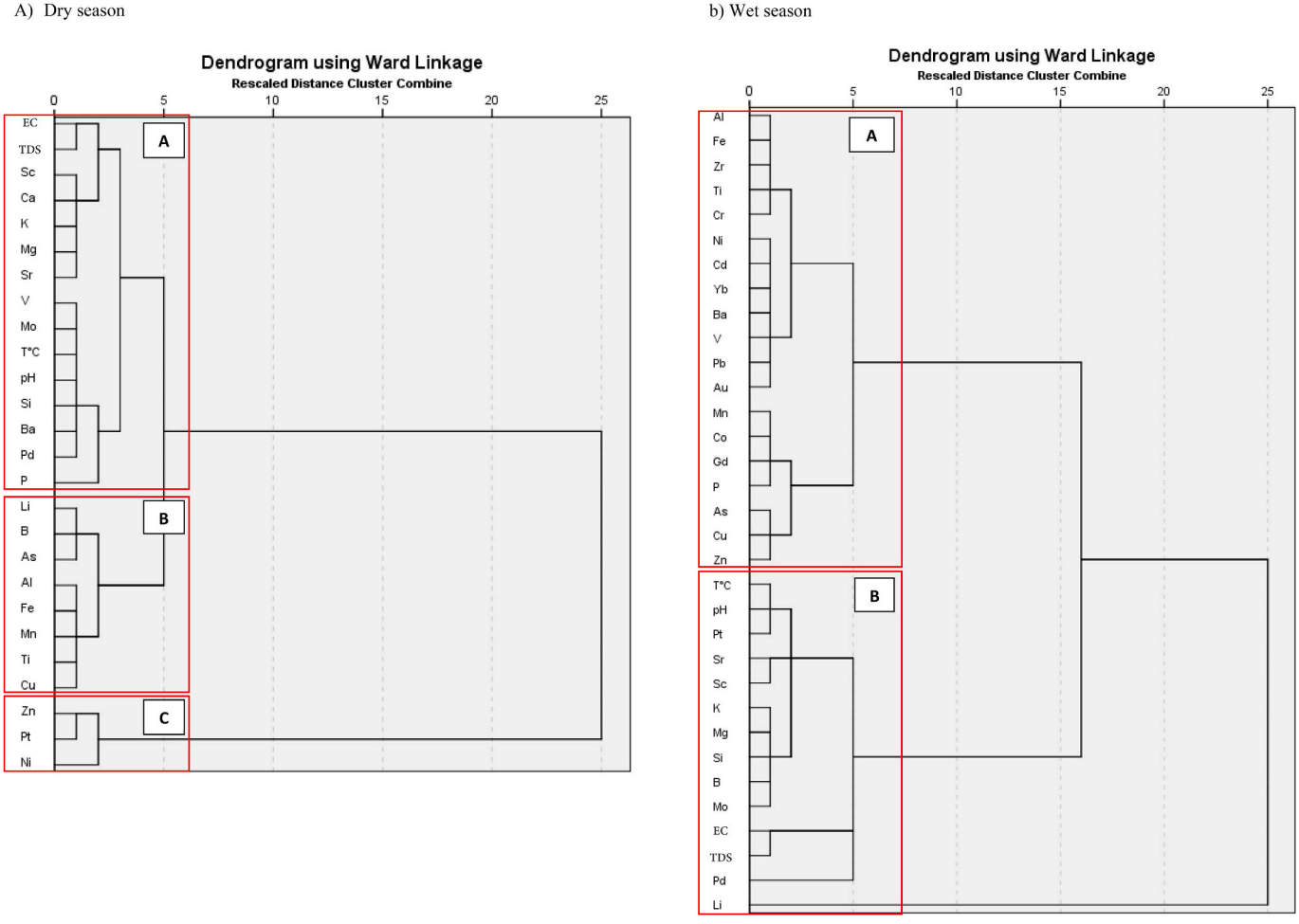

Fig. 4. Dendrogram showing cluster of metals and physical chemical parameters during the dry (a) and wet (b) seasons.

Table 6
Seasonal metal concentrations comparison with some regions in the world.

Country	Source	Metal	Concentration (μg L^{-1})		Reference
			Dry season	Wet season	
Pakistan	Mangla Lake	Cd	40.2	34.3	Saleem et al. (2019)
		Co	282	174	
		Cr	99.2	87.8	
		Cu	30.5	26.6	
		Fe	151	120	
		Mn	17.4	16.1	
		Ni	134	117	
		Pb	394	330	
		Sr	224	186	
		Zn	28.9	23.6	
India	Dhemaji district Groundwater	As	8	6	Buragohain et al. (2010)
		Pb	287	194	
		Cd	39	20	
		Al	3183	1824	
Republic of Ghana	Tano River	Pb	219	543	Nyantakyi et al. (2019)
		Cd	35	65	
		As	4	21	
		Cr	55	477	
		Zn	55	243	
Nigeria	Pompom River	Cd	0.01	0.05	Omono et al. (2014)
		Cu	0.01	0.09	
		Ni	0.01	0.01	
		Pb	0.01	0.01	
		Zn	0.03	0.04	
India	Sabarmati River	Pb	47–61	42–51	Kumar et al. (2013)
		Ni	34–35	0–24	
		Cr	5170–18600	0.028–0.093	
		Zn	76–78	85–86	
		Cu	36–56	13–14	
China	Taipu River	Ba	80	158	Yao et al. (2014)
		Cd	3	3	
		Cr	9	17	
		Cu	16	43	
		Fe	334	423	
		Mn	97	266	
		Ni	16	24	
		Pb	57	108	
		Zn	64	190	

6. Conclusions

The Andes cordillera is a natural rich source of many minerals. This feature, in convergence with marked season triggers, does result in seasonal variations of several important TM and metalloids in the aquatic ecosystems which are used extensively as sources of irrigation and drinking water. The results presented herein provide an initial indication of how seasonality affects the concentrations of 38 elements (22 regulated and 18 unregulated) in the southern basins around Arequipa. Further work is needed to fully understand the spatio-temporal dynamic of TMs and metalloids in the southern basins of Peru. In general, the concentrations and prevalence (i.e., number detected) of elements were higher near urbanized areas, and near the mouths of each basin. Total recoverable metals, rather than dissolved metal concentrations, trended better with season. In comparison to Peruvian and U.S. EPA water quality guidelines, Al, Fe, As, B, Mn, P, Pb, and Ni were found as potential pollutants of concern in all of the basins studied. The unregulated elements of strontium and lithium were detected at medium to high concentrations in all the basins. These two elements deserve more attention in future studies. Most monitored elements were found at comparatively higher concentrations during the wet season, compared to the dry season. Seasonal correlations strongly indicated higher concentrations of Al, Au, Ba, Cd, Co, Cu, Fe, Gd, Mn, Ni, P, Pb, Ti, Yb and Zr during high flows (85–350 m^3/s), with As, B, Ge, Li and Pd occurring at higher concentrations during low flows (5–40 m^3/s). The most affected basins, based on elements found at high concentrations, were in the following order: Tambo > Chili-Quilca > Camaná > Ocoña. The multivariate statistical technique, PCA, shed some light on probable sources during the dry and wet seasons. It appears that agricultural activities and natural soil weathering are predominant source of some elements during the dry season, whereas urban and industrial runoff, and natural soil oxidation processes influence the concentrations of some elements (e.g., iron and aluminum) during the wet season.

CRediT author contribution statement

Alexander Ccanccapa: Conceptualization, Data curation, Formal analysis, Investigation, Methodology, Validation, Visualization, Writing - original draft, Writing - review & editing; Betty Paredes: Conceptualization, Investigation, Methodology, Project administration, Supervision, Writing - review & editing; Corina Vera: Conceptualization, Investigation, Methodology, Project administration, Supervision, Writing - review & editing; Francisco D. Chavez-Gonzales, Guillermo Gutierrez, Roland Valencia, Ana Lucia Paz Alcázar, Nadezhda N. Zyaykina, Timothy R. Filley: Investigation, Methodology, Writing - review & editing; Chad T. Jafvert: Conceptualization, Project administration, Resources, Supervision, Funding acquisition, Methodology, Writing - review & editing.

Declaration of competing interest

The authors declare that they have no known competing financial interests or personal relationships that could have appeared to influence the work reported in this paper.

Data availability

Data will be made available on request.

Acknowledgements

The authors gratefully acknowledge this paper to be an outcome of a project which is part of the Arequipa Nexus Institute for Food, Energy, Water, and the Environment, with funding provided by the Universidad Nacional de San Agustin.

Appendix A. Supplementary data

Supplementary data to this article can be found online at https://doi.org/10.1016/j.jenvman.2023.118493.

References

Adams, W., Blust, R., Dwyer, R., Mount, D., Nordheim, E., Rodriguez, P.H., Spry, D., 2020. Bioavailability assessment of metals in freshwater environments: a historical review. Environ. Toxicol. Chem. 39, 48–59.
Allafta, H., Opp, C., 2020. Spatio-temporal variability and pollution sources identification of the surface sediments of Shatt Al-Arab River, Southern Iraq. Sci. Rep. 10, 6979.
Alvan, A., Decou, A., Mamani, M., 2012. Stratigraphic Characterization of Arequipa Basin from Sedimentary Stacking Pattern and Ammonite Biozones.
Alves, R.I.S., Machado, G.P., Zagui, G.S., Bandeira, O.A., Santos, D.V., Nadal, M., Sierra, J., Domingo, J.L., Segura-Muñoz, S.I., 2019. Metals risk assessment for children's health in water and particulate matter in a southeastern Brazilian city. Environ. Res. 177, 108623.
Barenys, M., Boix, N., Farran-Codina, A., Palma-Linares, I., Montserrat, R., Curto, A., Gomez-Catalan, J., Ortiz, P., Deza, N., Llobet, J.M., 2014. Heavy metal and metalloids intake risk assessment in the diet of a rural population living near a gold mine in the Peruvian Andes (Cajamarca). Food Chem. Toxicol. 71, 254–263.
Bashir, M.F., Ma, B.J., Bilal Komal, B., Bashir, M.A., Farooq, T.H., Iqbal, N., Bashir, M., 2020. Correlation between environmental pollution indicators and COVID-19 pandemic: a brief study in Californian context. Environ. Res. 187, 109652.
Bebbington, A.J., Bury, J.T., 2009. Institutional challenges for mining and sustainability in Peru. Proc. Natl. Acad. Sci. U. S. A. 106, 17296–17301.
Buragohain, M., Bhuyan, B., Sarma, H.P., 2010. Seasonal variations of lead, arsenic, cadmium and aluminium contamination of groundwater in Dhemaji district, Assam, India. Environ. Monit. Assess. 170, 345–351.
Cabrera, D.U.M., Caceres, E.A., Ramos, D.Z., Prado, J.F., Rodas, Z.L.M., Ventura, A.T., 2017. Arsenic total not desired to referential values of ph in surface water, sama hydrographic basin, Tacna-Peru region. Rev. Investig. Altoandinas-J. High Andean Res. 19, 305–312.
Caccia, V.G., Millero, F.J., 2003. The distribution and seasonal variation of dissolved trace metals in Florida bay and adjacent waters. Aquat. Geochem. 9, 111–144.
Ccanccapa-Cartagena, A., Paredes, B., Vera, C., Chavez-Gonzales, F.D., Olson, E.J., Welp, L.R., Zyaykina, N.N., Filley, T.R., Warsinger, D.M., Jafvert, C.T., 2021. Occurrence and probabilistic health risk assessment (PRA) of dissolved metals in surface water sources in Southern Peru. Environ. Adv. 5, 100102.
Chapman, D.V., World Health, O., Unesco, United Nations Environment, P., 1996. Water quality assessments: a guide to the use of biota, sediments and water in environmental monitoring/edited by Deborah Chapman, second ed. ed. E & FN Spon, London.
Chowdhury, S., Mazumder, M.A.J., Al-Attas, O., Husain, T., 2016. Heavy metals in drinking water: occurrences, implications, and future needs in developing countries. Sci. Total Environ. 569–570, 476–488.
Cosmas, U., 2011. Synergism between Season, pH, Conductivity and Total Dissolved Solids (TDS) of Imo River Quality for Agricultural Irrigation.
de Meyer, C.M.C., Rodríguez, J.M., Carpio, E.A., García, P.A., Stengel, C., Berg, M., 2017. Arsenic, manganese and aluminum contamination in groundwater resources of Western Amazonia (Peru). Sci. Total Environ. 607–608, 1437–1450.
DelValls, T.Á., Forja, J.M., González-Mazo, E., Gómez-Parra, A., Blasco, J., 1998. Determining contamination sources in marine sediments using multivariate analysis. TrAC, Trends Anal. Chem. 17, 181–192.
Fabre, A., Gauquelin, T., Vilasante, F., Ortega, A., Puig, H., 2006. Phosphorus content in five representative landscape units of the Lomas de Arequipa (Atacama Desert-Peru). Catena 65, 80–86.
Gałaś, A., 2014. Petrology and new data on the geochemistry of the Andahua volcanic group (Central Andes, southern Peru). J. S. Am. Earth Sci. 56, 301–315.
Gardner, C.B., Carey, A.E., 2004. Trace metal and major ion inputs into the olentangy river from an urban storm sewer. Environ. Sci. Technol. 38, 5319–5326.
Garreaud, R., 2009. The Andes climate and weather. Adv. Geosci. 22, 3–11.
Geological Survey, U.S.A., 2018. 2015 Minerals Yearbook.
Gozzard, E., Mayes, W.M., Potter, H.A.B., Jarvis, A.P., 2011. Seasonal and spatial variation of diffuse (non-point) source zinc pollution in a historically metal mined river catchment, UK. Environ. Pollut. 159, 3113–3122.
Grande, J.A., Loayza-Muro, R., Alonso-Chaves, F.M., Fortes, J.C., Willems, B., Sarmiento, A.M., Santisteban, M., Dávila, J.M., de la Torre, M.L., Durães, N., Diaz-Curiel, J., Luís, A.T., 2019. The Negro River (Ancash-Peru): a unique case of water pollution, three environmental scenarios and an unresolved issue. Sci. Total Environ. 648, 398–407.
Guittard, A., Baraer, M., McKenzie, J.M., Mark, B.G., Rapre, A.C., Bury, J., Carey, M., Young, K.R., 2020. Trace metal stream contamination in a post peak water context: lessons from the cordillera Blanca, Peru. ACS Earth Space Chem 4, 506–514.
Gundersen, P., Steinnes, E., 2001. Influence of temporal variations in river discharge, pH, alkalinity and Ca on the speciation and concentration of heavy metals in some mining polluted rivers. Aquat. Geochem. 7, 173–193.
Hossain, M.S., Ahmed, M.K., Sarker, S., Rahman, M.S., 2020. Seasonal variations of trace metals from water and sediment samples in the northern Bay of Bengal. Ecotoxicol. Environ. Saf. 193, 110347.
Hudson-Edwards, K.A., Archer, J., 2012. Geochemistry of As-, F- and B-bearing waters in and around San Antonio de los Cobres, Argentina, and implications for drinking and irrigation water quality. J. Geochem. Explor. 112, 276–284.
Jiajun, H., Huimin, Z., Hui, Z., Xuan, G., Mingwei, S., Junhao, Z., Xiaotao, L., 2014. Ecological risk and economic loss estimation of heavy metals pollution in the beijiang river. Ecol. Chem. Eng. S 21, 189–199.
Kumar, R.N., Solanki, R., Kumar, J.I.N., 2013. Seasonal variation in heavy metal contamination in water and sediments of river Sabarmati and Kharicut canal at Ahmedabad, Gujarat. Environ. Monit. Assess. 185, 359–368.
Kumar, V., Parihar, R.D., Sharma, A., Bakshi, P., Singh Sidhu, G.P., Bali, A.S., Karaouzas, I., Bhardwaj, R., Thukral, A.K., Gyasi-Agyei, Y., Rodrigo-Comino, J., 2019. Global evaluation of heavy metal content in surface water bodies: a meta-analysis using heavy metal pollution indices and multivariate statistical analyses. Chemosphere 236, 124364.
Lavado Casimiro, W.S., Ronchail, J., Labat, D., Espinoza, J.C., Guyot, J.L., 2012. Basin-scale analysis of rainfall and runoff in Peru (1969–2004): Pacific, Titicaca and Amazonas drainages. Hydrol. Sci. J. 57, 625–642.
Le Pape, P., Quantin, C., Morin, G., Jouvin, D., Kieffer, I., Proux, O., Ghanbaja, J., Ayrault, S., 2014. Zinc speciation in the suspended particulate matter of an urban river (orge, France): influence of seasonality and urbanization gradient. Environ. Sci. Technol. 48, 11901–11909.
Li, F., Wen, Y.M., Zhu, P.T., 2008. Bioavailability and toxicity of heavy metals in a heavily polluted river, in PRD, China. Bull. Environ. Contam. Toxicol. 81, 90–94.
Li, S., Zhang, Q., 2010. Risk assessment and seasonal variations of dissolved trace elements and heavy metals in the Upper Han River, China. J. Hazard Mater. 181, 1051–1058.
Liu, G.Q., Lao, Q.B., Su, Q.Z., Shen, Y.L., Chen, F.J., Qing, S.M., Wei, C.L., Zhang, C.H., 2019a. Spatial and seasonal characteristics of dissolved heavy metals in the aquaculture areas of Beibu Gulf, South China. Human Ecol. Risk Assess. 26, 1957–1969.
Liu, R., Guo, L., Men, C., Wang, Q., Miao, Y., Shen, Z., 2019b. Spatial-temporal variation of heavy metals' sources in the surface sediments of the Yangtze River Estuary. Mar. Pollut. Bull. 138, 526–533.
Lynam, D.R., Pfeifer, G.D., Fort, B.F., Gelbcke, A.A., 1990. Environmental assessment of MMT™ fuel additive. Sci. Total Environ. 93, 107–114.
Mansoor, S.Z., Louie, S., Lima, A.T., Van Cappellen, P., MacVicar, B., 2018. The spatial and temporal distribution of metals in an urban stream: a case study of the Don River in Toronto, Canada. J. Great Lake. Res. 44, 1314–1326.
Maos, J.O., 1985. Water resource development and land settlement in Southern Peru: the Majes Project. Geojournal 11, 69–78.
Masscheleyn, P.H., Delaune, R.D., Patrick, W.H., 1991. Effect of redox potential and pH on arsenic speciation and solubility in a contaminated soil. Environ. Sci. Technol. 25, 1414–1419.
Millas, I.G., 2020. Boron Industry, Sources, and Evaporitic Andean Deposits: Geochemical Characteristics and Evolution Paths of the Superficial Brines.
MINAM, 2017. In: Ambiente, M.d.M. (Ed.), Estándares de Calidad Ambiental (ECA) para Agua N° 004-2017-MINAM. Lima.
Ministerio de Enegia y Minas, P., 2019. In: ESTAMIN (Ed.), Boletin Estistico Minero. Ministerio de Enegia y Minas, Perú, pp. 1–32.
Mohiuddin, K.M., Otomo, K., Ogawa, Y., Shikazono, N., 2012. Seasonal and spatial distribution of trace elements in the water and sediments of the Tsurumi River in Japan. Environ. Monit. Assess. 184, 265–279.
Montesinos-Tubée, D.B., Nuñez del Prado, H., Toni, B., Alvarez, E., Lozada, A., Flores, J., Paco, G., Maldonado Fonkén, M.S., Moscoso, M., Riveros Arteaga, C., Tamayo, D., 2019. Floristic diversity, plant communities and conservation proposals of the riparian forest in the Chili River (Arequipa, Peru). Arnaldoa 26, 97–130.
Nguyen, B.T., Do, D.D., Nguyen, T.X., Nguyen, V.N., Phuc Nguyen, D.T., Nguyen, M.H., Thi Truong, H.T., Dong, H.P., Le, A.H., Bach, Q.-V., 2020. Seasonal, spatial variation, and pollution sources of heavy metals in the sediment of the Saigon River, Vietnam. Environ. Pollut. 256, 113412.
Nieto, B.V.G.F.d., 2019. Contaminación del Agua por Metales Pesados As, B, Cu, Pb, Cd y CN-en las Cuencas de los Ríos Tambo, Quilca, Camaná y Ocoña de la Región Arequipa Facultad de Ciencias Naturales y Formales. Universidad Nacional de San Agustin, Arequipa.
Nthunya, L.N., Masheane, M.L., Malinga, S.P., Nxumalo, E.N., Mamba, B.B., Mhlanga, S. D., 2017. Determination of toxic metals in drinking water sources in the chief Albert luthuli local municipality in mpumalanga, South Africa. Phys. Chem. Earth, Parts A/B/C 100, 94–100.
Nyantakyi, A.J., Akoto, O., Fei-Baffoe, B., 2019. Seasonal variations in heavy metals in water and sediment samples from river Tano in the bono, bono East, and Ahafo regions, Ghana. Environ. Monit. Assess. 191.
Omono, C., Amune, M., Kakulu, S., 2014. Seasonal variations in dissolved heavy metals in Pompom River, Itakpe, Nigeria. Pak. J. Sci. Ind. Res. Ser. A: Phys. Sci. 57, 40–46.
Organization, W.H., 2009. Boron in Drinking-Water. Switzerland.

Pari-Huaquisto, D.C., Alfaro-Alejo, R., Pilares-Hualpa, I., Belizario, G., 2020. Seasonal variation of heavy metals in surface water of the Ananea river contaminated by artisanal mining, Peru. IOP Conf. Ser. Earth Environ. Sci. 614, 012167.
Perry, L.B., Seimon, A., Kelly, G.M., 2014. Precipitation delivery in the tropical high Andes of southern Peru: new findings and paleoclimatic implications. Int. J. Climatol. 34, 197–215.
Pizarro, J., Vergara, P.M., Rodríguez, J.A., Valenzuela, A.M., 2010. Heavy metals in northern Chilean rivers: spatial variation and temporal trends. J. Hazard Mater. 181, 747–754.
Reza, R., Singh, G., 2010. Heavy metal contamination and its indexing approach for river water. Int. J. Environ. Sci. Technol. 7, 785–792.
Rusydi, A., 2018. Correlation between conductivity and total dissolved solid in various type of water: a review. IOP Conf. Ser. Earth Environ. Sci. 118, 012019.
Saleem, M., Iqbal, J., Shah, M.H., 2019. Seasonal variations, risk assessment and multivariate analysis of trace metals in the freshwater reservoirs of Pakistan. Chemosphere 216, 715–724.
Schaefer, M.V., Ying, S.C., Benner, S.G., Duan, Y., Wang, Y., Fendorf, S., 2016. Aquifer arsenic cycling induced by seasonal hydrologic changes within the Yangtze River Basin. Environ. Sci. Technol. 50, 3521–3529.
Sepulchre, P., Sloan, L.C., Snyder, M., Fiechter, J., 2009. Impacts of Andean uplift on the Humboldt Current system: a climate model sensitivity study. Paleoceanography 24.
Singh, U.K., Kumar, B., 2017. Pathways of heavy metals contamination and associated human health risk in Ajay River basin, India. Chemosphere 174, 183–199.
Standen, V.G., Santoro, C.M., Arriaza, B., Valenzuela, D., Coleman, D., Monsalve, S., 2018. Prehistoric polydactylism: biological evidence and rock art representation from the Atacama Desert in northern Chile. International Journal of Paleopathology 22, 54–65.
Stets, E.G., Kelly, V.J., Crawford, C.G., 2014. Long-term trends in alkalinity in large rivers of the conterminous US in relation to acidification, agriculture, and hydrologic modification. Sci. Total Environ. 488–489, 280–289.
Terrazas, E.M., Perez, G.A., Tapia, R.A., Saavedra, M.A., Limachi, S.A., Camacho, G.G., 2017. Interactive determination by total metals in waters of inner Puno bay the Lake Titicaca-Peru. Rev. Investig. Altoandinas-J. High Andean Res. 19, 125–134.
Tilton, G.R., Barreiro, B.A., 1980. Origin of lead in andean calc-alkaline lavas, southern Peru. Science 210, 1245–1247.
UNESCO, 2006. In: Caribe, O.R. (Ed.), Balance hídrico superficial del Perú a nivel multianual. Montevideo, Uruguay.
USEPA, 2009. National primary drinking water regulations. In: Office of Water. U.S.E.P. A. (Ed.), Washington DC.
Varol, M., 2013. Temporal and spatial dynamics of nitrogen and phosphorus in surface water and sediments of a transboundary river located in the semi-arid region of Turkey. Catena 100, 1–9.
Vera, D.I.S., 2017. Evaluación y Mejoramiento de la Planta de Tratamiento de Agua Hernan Perochena-Mollendo, Health Engineering. Universidad Nacional de San Agustin de Arequipa, Arequipa, Peru, p. 262.
Viale, M., Bianchi, E., Cara, L., Ruiz, L.E., Villalba, R., Pitte, P., Masiokas, M., Rivera, J., Zalazar, L., 2019. Contrasting climates at both sides of the Andes in Argentina and Chile. Front. Environ. Sci. 7.
Vukovic, D., Vukovic, Z., Stankovic, S., 2014. The impact of the Danube Iron Gate Dam on heavy metal storage and sediment flux within the reservoir. Catena 113, 18–23.
Walaszek, M., Bois, P., Laurent, J., Lenormand, E., Wanko, A., 2018. Urban stormwater treatment by a constructed wetland: seasonality impacts on hydraulic efficiency, physico-chemical behavior and heavy metal occurrence. Sci. Total Environ. 637–638, 443–454.
Wang, H., Sun, L., Liu, Z., Luo, Q., 2017. Spatial distribution and seasonal variations of heavy metal contamination in surface waters of Liaohe River, Northeast China. Chin. Geogr. Sci. 27, 52–62.
Wang, X., Zhao, L., Xu, H., Zhang, X., 2018. Spatial and seasonal characteristics of dissolved heavy metals in the surface seawater of the Yellow River Estuary, China. Mar. Pollut. Bull. 137, 465–473.
Xiaolong, W., Jingyi, H., Ligang, X., Qi, Z., 2010. Spatial and seasonal variations of the contamination within water body of the Grand Canal, China. Environ. Pollut. 158, 1513–1520.
Yacoub, C., Blazquez, N., Perez-Foguet, A., Miralles, N., 2013. Spatial and temporal trace metal distribution of a Peruvian basin: recognizing trace metal sources and assessing the potential risk. Environ. Monit. Assess. 185, 7961–7978.
Yao, H., Qian, X., Gao, H., Wang, Y., Xia, B., 2014. Seasonal and spatial variations of heavy metals in two typical Chinese rivers: concentrations, environmental risks, and possible sources. Int. J. Environ. Res. Publ. Health 11, 11860–11878.
Zehetner, F., Miller, W.P., 2006. Erodibility and runoff-infiltration characteristics of volcanic ash soils along an altitudinal climosequence in the Ecuadorian Andes. Catena 65, 201–213.
Zhang, J.-W., Yan, Y.-N., Zhao, Z.-Q., Li, X.-D., Guo, J.-Y., Ding, H., Cui, L.-F., Meng, J.-L., Liu, C.-Q., 2020. Spatial and seasonal variations of dissolved arsenic in the Yarlung Tsangpo River, southern Tibetan Plateau. Sci. Total Environ., 143416